Neuronal IL-17 controls *C. elegans* developmental diapause through p53/CEP-1

Abhishiktha Godthi[1], Srijit Das[1], Johnny Cruz-Corchado[1], Andrew Deonarine[1], Kara Misel-Wuchter[2], Priya D. Issuree[2] and Veena Prahlad[1, 3, *]

Affiliations: [1]Department of Biology,

338 Biology Building East,

143 Biology Building, Iowa City, IA 52242-1324.

[2]Department of Internal Medicine,

503 Eckstein Medical Research Building,

431 Newton Road, Iowa City, IA 52242

[3]Iowa Neuroscience Institute

169 Newton Road, 2312 Pappajohn Biomedical Discovery Building

Iowa City, IA 52242

***** Corresponding author email**:** **veena-prahlad@uiowa.edu**

Abstract: Metazoan growth and development requires the coordination of cell cycle progression and metabolism with nutrient availability[1-3]. Here, we show that in *C. elegans*, amphid neurons regulate the animals' developmental decision to continue reproductive growth or arrest as quiescent dauer larvae in response to food, by controlling the activity of *C. elegans* p53-like ortholog, CEP-1. Specifically, upon food availability, larval neurons secrete a mammalian IL-17 ortholog, ILC-17.1, and ILC-17.1 signaling is needed for *C. elegans* to progress through development into reproductive adults. ILC-17.1 deficiency activates CEP-1/p53 in larval blast cells, and causes larvae to arrest as stress-resistant, quiescent dauers by activating DAF-16/FOXO, decreasing cytochrome C levels, decreasing glucose utilization, and upregulating cell cycle inhibitors. Increasing ILC-17.1 levels represses CEP-1/p53 and promotes anabolic growth, but also inhibits apoptosis upon genotoxic stress. IL-17 also represses p53 in human epithelial cells. These studies describe a role for the tumor suppressor p53-like proteins in controlling developmental quiescence of a metazoan in response to neuronal activity and immunometabolic signals and are relevant to our understanding of neuroimmune mechanisms in cancer. This novel role for p53-like proteins in *C. elegans* supports the argument that their developmental function was a main driving force in their evolution[4,5].

Main

During the development of a multicellular organism, nutrient availability is coordinated with the division, growth and metabolic activity of cells through cell-cell communication[6]. Cytokines are a group of secreted proteins that coordinate communication between immune and non-immune cells through paracrine or endocrine signaling mechanisms[7,8]. The IL-17 cytokines are an evolutionarily conserved family of proinflammatory cytokines released by specialized immune cells, at sites such as epithelia that serve as an interface between the organism and the outside world[9,10]. In humans, IL-17 cytokines act on IL-17 receptor expressing cells to activate immune surveillance, barrier function and wound healing, but can trigger autoimmune conditions such as psoriasis and multiple sclerosis and contribute to the growth and metastasis of cancers[9,11-13]. In *C. elegans* too, one of three of IL-17 orthologs[14,15], ILC-17.1 is expressed by cells with epithelial properties, i.e. by a subset of specialized neurons called amphid neurons that sense information from the environment[16,17].

Here we show that ILC-17.1 is secreted upon exposure to food and controls CEP-1, the *C. elegans* ortholog of the mammalian tumor suppressor p53, to coordinate cell cycle progression and glucose utilization with food availability during *C. elegans* development. ILC-17.1 is necessary to repress CEP-1/p53 and allow *C. elegans* larvae to progress through development into reproductive adults. In the absence of ILC-17.1, CEP-1/p53 is activated, accumulates in progenitor blast cells of larvae, and alters the expression of cell cycle inhibitors and metabolic enzymes, causing larvae to arrest growth and development in an alternative, hypometabolic, quiescent state called dauer.

The p53-like tumor suppressor genes are found in all multicellular animals, where they prevent the propagation of damaged DNA by triggering apoptosis of germ line cells that accrue DNA damage, thus maintaining the fidelity of the species [4,5,18,19]. This function of the p53-family of

proteins is thought to be the main driving force in their evolution. This is largely because, although p53-like genes affect vertebrate development[4,5,18], cell competition[20,21], and stem cell differentiation[22,23] through as yet poorly understood mechanisms, in invertebrates such as *D. melanogaster* and *C. elegans* the function of the p53-gene family has been restricted to regulating apoptosis. Here we show, for the first time, a novel role for CEP-1/p53 in controlling developmental quiescence of *C. elegans*. Our studies showing that CEP-1/p53 acts to switch metazoan development between continuous growth and dormancy, support an alternative possibility that the role of p53-like proteins in coordinating cell quiescence with metabolism during development in response to environmental signals, could have shaped the evolution of this important gene family[24].

ILC-17.1 is secreted from *C. elegans* amphid neurons in response to food and prevents dauer arrest.

C. elegans is a bacterivore. When *C. elegans* larvae hatch under optimal conditions (e.g., in the laboratory at 20°C, on abundant food provided by lawns of *E. coli* strain, OP50) they progress through development and become reproductive adults. However, if they hatch under suboptimal conditions, such as in the paucity of food, at high population densities, or high ambient temperatures, larvae implement an alternative developmental decision to arrest growth as quiescent, stress resistant, dauer larvae adapted for dispersal. Animals then resume development when conditions are favorable again[25,26]. We discovered that a deletion of *ilc-17.1,* syb5296*,* that removes almost all the coding sequence (2188 bp of 2980 bp; Supplementary Fig. S1a) and abolishes mRNA expression (Supplementary Fig. S1b) caused larvae to constitutively enter the dauer state even under optimal growth conditions (Supplementary Fig. S1c-d). Dauer larvae can be identified by their distinct morphology, growth arrest, and resistance to detergent (1% SDS) due to changes in their cuticle and the presence of a buccal plug that inhibits ingestion [26]. Approximately 30% (31.2 ±5%) of *ilc-17.1*(syb5296) X larvae were SDS-resistant 48 hours post-

hatching on OP50 at 20°C (Supplementary Fig. S1 c, d). In contrast, under the same conditions, none of the wildtype larvae were detergent resistant, nor did they arrest as dauers (Supplementary Fig. S1c, d). Under these optimal conditions, dauer entry of the *ilc-17.1* deleted larvae was transient and most larvae exited dauer within 72 hours and continued development to become reproductive adults, also confirmed by their susceptibility to 1% SDS (Supplementary Fig. S1c, d). However, as with other mutations that promote dauer entry[25-27], the dauer arrest of *ilc-17.1* deletion mutants persisted at the slightly more stressful ambient temperature of 25°C, which still supported the growth of wild-type animals into reproductive adults, but caused practically all larvae lacking *ilc-17.1* to enter and remain arrested as dauer larvae (Fig.1a-c; Supplementary Fig. S1e).

As previously reported, *ilc-17.1* mRNA is expressed only in amphid neurons[14], which we confirmed by expressing mCherry as a bicistronic SL2 cassette along with the endogenous *ilc-17.1* gene to report on sites of *ilc-17.1* expression (Supplementary Fig. S1f). The dauer phenotype could be rescued by re-expressing *ilc-17.1* in *ilc-17.1* deletion mutants, under the control of its own promoter and 3' UTR regions (Fig.1b, expression levels of rescue constructs in Supplementary Fig. S1g). To determine whether ILC-17.1 acted in a paracrine or endocrine manner to promote continuous development, we also expressed ILC-17.1 ectopically in the body wall muscle cells of *ilc-17.1* deleted larvae, under the *unc-54* promoter, (Supplementary Fig. S1g, h) and asked whether this could rescue the dauer phenotype of these deletion mutants. This was the case (Fig.1b), and in fact, ectopic ILC-17.1 expressed at two-fold higher levels from the muscle promoter than from the endogenous promoter (Supplementary Fig. S1g), prevented a larger fraction of *ilc-17.1* deletion mutant larvae from arresting as dauers (Fig.1b). Thus, it appeared that ILC-17.1 was likely secreted to exert its systemic effects.

IL-17 cytokines signal through cytokine receptors[9] which in *C. elegans* are encoded by the *ilcr-1* and *ilcr-2* genes[14], and the ILCR-2 receptor is expressed in practically all tissues, also determined using a bicistronic SL2 cassette to tag the *ilcr-2* receptor at its endogenous locus with GFP (Supplementary Fig. S1i). RNAi mediated downregulation of *ilcr-2* reduced the percentage of *ilc-17.1* larvae that were rescued from dauer arrest by overexpressing ILC-17.1 in the muscle, indicating that ectopic ILC-17.1 acted through the ILCR-2 receptors to promote continuous development (Fig. 1d). More importantly, *ilcr-2* downregulation through RNAi caused approximately half (51.05 ± 9%) of the wild-type (N2) animals to arrest as dauers (Fig. 1d). Together, these observations indicated that during normal development, ILC-17.1 signaling through the ubiquitously expressed ILCR-2 receptors was required for growth of larvae to reproducing adults; in the absence of ILC-17.1, larvae arrested growth and entered the dauer state, transiently, or for prolonged durations.

Because the dauer diapause decision is made during the first two larval stages, and because nutrient availability is a major factor in the dauer decision[25,26], we asked whether ILC-17.1 was normally secreted by larvae in response to food. To do this we immunolocalized ILC-17.1 protein in *C. elegans* larvae expressing endogenous HA-tagged ILC-17.1 and examined its tissue distribution in the presence or absence of food (Fig. 1e). While *ilc-17.1* mRNA expression remained restricted to the amphid neurons both in the presence and absence of food, as detected by mCherry expression (Fig. 1e; left), ILC-17.1 protein was present outside the amphid neurons in the pharynx when larvae were exposed to food (OP50), but not when larvae hatched in the absence of food (Fig.1e; right). In addition, ectopically expressed ILC-17.1 protein, even when expressed under a muscle-specific promoter (Supplementary Fig. S1h), could be detected throughout the animal, outside muscle cells, at neurons and other tissue (Supplementary Fig.S1j), confirming that ILC-17.1 could indeed be secreted under normal conditions, to act systemically and promote the continuous development of larvae.

RNA-seq analysis of total RNA extracted from bleach synchronized larvae grown for 30-34 hours at 25°C confirmed that, as might be expected of larvae entering dauer diapause[28,29], *ilc-17* deleted larvae had downregulated anabolic processes and upregulated catabolic processes (Supplementary Fig. S2, a-c; Supplementary Table 1-3). Thus, DNA replication and ribosome biogenesis were downregulated when compared to wild-type animals, or larvae rescued from dauer arrest by *ilc-17.1* overexpression in muscle cells (Supplementary Fig. S2b;). On the other hand, autophagy, fatty acid metabolism, and stress responses such as glutathione metabolism and xenobiotic defense pathways were upregulated (Supplementary Fig. S2c). At this time point, *ilc-17.1* mutant larvae were not phenotypically identifiable as dauers although the dauer decision would have been made [30,31] and wild-type larvae were in late larval stage 2 (L2) or early larval stage 3 (L3) of development. To evaluate the extent to which the *ilc-17.1* deleted dauers were similar to previously described *C. elegans* dauers that accumulate in the population upon starvation, we compared the gene expression changes in *ilc-17.1* mutant larvae *en route* to arrest as dauers, with previously published gene expression changes in dauer larvae collected from starved plates[32] (Supplementary Fig. S2 d). Indeed, the global gene expression profile of *ilc-17.1* deletion mutants as they entered dauer was significantly, although modestly, correlated with the gene expression changes in dauer larvae obtained upon starvation (Supplementary Fig. S2d; Supplementary Table 4). Dauer larvae are known to upregulate specific collagen genes that differ from the collagens expressed by larvae undergoing continuous development[33]. The increase in expression of these specific dauer- signature collagen genes was recapitulated in *ilc-17.1* larvae during dauer entry (Supplementary Fig. S2 e).

Given the previously described role of ILC-17.1 as a neuromodulator[14] we first suspected that the secretion of ILC-17.1 functioned to modulate the animals' sensory perception of food, or their feeding behavior. However, we found no evidence to support this (Supplementary Fig. S3): *ilc-*

147 *17.1* deleted animals did not exhibit changes in chemotaxis towards lawns of OP50, or towards
148 organic molecules like lysine or diacetyl thought to mimic the presence of bacteria
149 (Supplementary Fig. S3a). Animals lacking ILC-17.1 were also able to feed like wild-type animals,
150 and the rate of pharyngeal pumping, a measure that is typically correlated with food uptake, was
151 the same in wild-type animals and animals lacking ILC-17.1, both in the presence and absence
152 of food (Supplementary Fig. S3b). Also, prior to their dauer entry, *ilc-17.1* deletion mutants
153 accumulated slightly, but not significantly fewer numbers of red latex beads in their intestinal
154 lumen that served as a proxy for rates of bacterial ingestion (Supplementary Fig. S3c). These
155 data suggested that *ilc-17.1* deficient larvae arrested development and entered a dauer diapause
156 state despite being able to ingest nutrients.
157
158 In mammals, cytokines regulate facilitated glucose uptake into cells by glucose transporters[34-38].
159 Likewise, in *C. elegans* ILC-17.1 was also required for larvae to utilize the normal amounts of
160 glucose available through their diets. Thus, while almost all *ilc-17* deletion larvae arrested as
161 dauers on normal diets of OP50, half or more larvae could escape dauer arrest and grow into
162 reproductive adults if their diets were supplemented with extra glucose (Fig. 1f; Supplementary
163 Fig. S4a). Importantly, no rescue from dauer was observed on the non-hydrolyzable glucose
164 analog 2-Deoxy-d-glucose (2-DOG; Fig. 1f) which cannot undergo glycolysis and does not enter
165 the metabolic pathway, suggesting that utilization of the supplemented glucose was required for
166 the rescue. In further support that glucose utilization was responsible for the dauer rescue, as
167 opposed to other non-specific effects of glucose, we found that the glucose rescue was not
168 inhibited by the mitochondria-targeted antioxidant, Mito-Tempo, that scavenges mitochondrial
169 reactive oxygen species, ROS, known to be increased under glucose-rich diets[39,40]
170 (Supplementary Fig. S4b). Nor was the rescue a non-specific effect of nutritional supplementation,
171 as L-glutamine, another important carbon source for metabolism[41], or skim milk powder that can
172 be ingested by *C.* elegans[41], did not suppress the dauer arrest of *ilc-17.1* larvae (Supplementary

Fig. S4c). Moreover, RNAi mediated downregulation of *fgt-1* the main glucose transporter (GLUT) responsible for glucose absorption in *C. elegans*[42] decreased the percentage of *ilc-17.1* deletion mutants that were rescued from dauer arrest by glucose supplementation (Supplementary Fig. S4d). Thus, even though *ilc-17.1* deletion mutants expressed normal mRNA levels of the putative GLUT orthologs including *fgt-1* (Supplementary Fig. S4e), the lack of ILC-17.1 was in some way decreasing glucose utilization by *ilc-17.1* larvae compared to wild-type animals.

These data together suggested that ILC-17.1 was not required for animals to find food, but its secretion signaled the presence of food in wild-type animals and was required to promote glucose utilization by the animal to support their growth. The lack of ILC-17.1, somehow, prevented continued development and instead activated a developmental switch that prompted *C. elegans* to arrest development as hypometabolic, stress resistant, dauer stage larvae.

ILC-17.1 loss activates CEP-1/p53 to induce DAF-16/FOXO and trigger dauer arrest.

In *C. elegans*, signal transduction pathways that predispose larvae to arrest as dauers, converge on the activation of the forkhead box transcription factors class O (FOXO) homolog, DAF-16[25,43-46]. Indeed, DAF-16 was activated in *ilc-17.1* deletion mutant larvae. This could be quantified by an increase in the number of DAF-16::GFP positive nuclei in the intestine of the *ilc-17.1* deletion mutants even at 20°C (Fig.1g), and the upregulation of DAF-16 target genes in *ilc-17.1* larvae, both at 20°C (Supplementary Fig. S5a) and 25°C (Fig.1h). Furthermore, a *daf-16* mutation, mu86, completely suppressed the dauer entry of animals lacking ILC-17.1 and abrogated the upregulation of *daf-16* targets genes, confirming that DAF-16 activation was responsible for their dauer entry (Supplementary Fig. S5a, Fig.1h, Fig. 1i, j).

Insulin signaling is one of the main mechanisms that promotes glucose uptake into cells, and reduced insulin signaling decreases glucose utilization and activates DAF-16 in *C.*

elegans[25,43,44,47]. However, ILC-17.1 did not appear to be acting through the insulin signaling pathway to activate DAF-16, as supported by the following observations: (i) expression levels of the insulin receptor *daf-2* mRNA did not differ between *ilc-17.1* deletion mutants, wild-type animals, and rescued *ilc-17.1* deletion mutants (Supplementary Fig. S5b; boxed; Supplementary Table 5), (ii) the dauer arrest of a mutation in the insulin receptor, *daf-2*(e1370), could not be rescued by ILC-17.1 overexpression, indicating that ILC-17.1 was not acting downstream of the insulin receptor (Supplementary Fig. 5c), (iii) the expression levels of the 28 insulin ligands including the three main insulins, *ins-4*, *ins-6* and *daf-28,* whose downregulation promotes dauer arrest [48,49], were not decreased, and *ins-4* mRNA levels were even slightly higher in *ilc-17.1* deleted larvae compared to wild-type animals (Supplementary Fig. S5b, d), (iv) the expression of *ins-1* and *ins-18* [47,48,50], whose upregulation has been shown to antagonize *daf-2* signaling and increase dauer propensity, were not increased (Supplementary Fig. S5b; arrows), (v) the expression of insulin peptides INS-4 and DAF-28 themselves were also not altered in larvae deficient in *ilc-17.1*, as seen using larvae expressing a GFP translational reporter of these insulin ligands (Supplementary Fig. S5e, f).

Since AMP-activated protein kinase (APMK) can be activated by glucose starvation[51,52] and can, in turn, activate DAF-16, we asked whether AMPK activation was responsible for the dauer arrest. However, knocking down the AMPK subunits *aak-1*, or *aak-2* or the *C. elegans* LKB1 homolog *par-4*, required for phosphorylation of AMPK did not rescue the dauer phenotype of *ilc-17.1* mutants (Supplementary Fig. S6a). In addition, Phopho-AMPK (Thr172)[53] levels were not higher in *ilc-17.1* mutant larvae prior to their dauer entry compared to wild-type larvae as determined by Western blot analysis (Supplementary Fig. S6b), suggesting that notwithstanding their decreased glucose metabolism, AMPK was unlikely to be responsible for the dauer arrest in *ilc-17.1* deletion mutants.

In *C. elegans,* pathways that modulate dauer have been extensively characterized. Therefore, to identify the mechanism(s) in *ilc-17.1* deleted larvae that led to DAF-16 activation, decreased glucose utilization and dauer arrest, we conducted RNAi to downregulate other known signaling pathways that could interact with DAF-16[54-58], or influence dauer formation, and assessed whether they rescued the dauer phenotype (Supplementary Fig. S6a). However, RNAi mediated modulation of most of the obvious pathways had little to no effect. For instance, decreasing *jnk-1* did not rescue dauer arrest of the *ilc-17.1* deleted animals (Supplementary Fig. S6a). Neither did RNAi mediated decrease nor increase of SKN-1 activity, the *C. elegans* ortholog of the mammalian Nrf1/2/3 (NF-E2-related factor) proteins[59]. HIF-1 levels were slightly higher in *ilc-17.1* animals (Supplementary Fig. S6c); however, the downregulation of *hif-1* or its negative regulators, *vhl-1,* and *egl-9*, did not suppress the dauer arrest (Supplementary Fig. S6a). For these experiments we used *daf-16* RNAi as a positive control. We therefore proceeded to test less well-characterized DAF-16-interactors in *C. elegans* [60-63]. Remarkably, amongst these, the deletion in *cep-1*, the *C. elegans* ortholog of p53[34,60,64,65] completely rescued the dauer arrest of *ilc-17.1* deletion mutants and nearly all (98%) of *ilc-17.1*(syb5296) X*; cep-1*(gk138) I double mutant larvae grew into reproductive adults, suggesting that CEP-1/p53 was activated in the absence of ILC-17.1 to trigger dauer arrest (Fig. 2a).

Although p53 is best studied as a tumor suppressor, p53-like proteins modulate vertebrate development through as yet poorly understood mechanisms[4,5,18,19,23]. The *C. elegans* p53 ortholog, *cep-1* has not been previously implicated in *C. elegans* development[65]. Nevertheless, consistent with the dauer rescue of *ilc-17.1* larvae upon *cep-1* deletion, the overexpression of CEP-1 alone was sufficient to arrest growth and promote an almost completely penetrant dauer phenotype in larvae that developed at 25°C (Fig. 2b, c; see Supplementary Fig. S6d for mRNA levels upon *cep-1* overexpression). CEP-1 overexpression was achieved by expressing a functional, fluorescently tagged CEP-1, CEP-1::GFP, that was able to complement a *cep-1*

deletion, *cep-1*(*lg12501*), [66-68] as a genomically integrated multicopy array in a wildtype background. CEP-1/p53 overexpression not only caused dauer arrest at 25°C, but also prompted larvae to transiently enter dauer at 20°C, as seen by their SDS-resistance, phenocopying the *ilc-17.1* deletion (Supplementary Fig. S6e). Like in the ILC-17.1 deficient animals, the dauer arrest of larvae overexpressing CEP-1 was also dependent on DAF-16: downregulating *daf-16* expression by RNAi rescued the dauer arrest caused by CEP-1/p53 overexpression (Fig. 2c), and *daf-16* target genes were upregulated in larvae overexpressing CEP-1/p53 (Fig 2e). Most convincing, the upregulation of *daf-16* target genes in *ilc-71.1* deletion mutant larvae was *cep-1* dependent at both 25°C and 20°C (Fig 2e; Supplementary Fig. S6f). CEP-1/p53 induced dauer entry appeared to be somewhat specific to reduced ILC-17.1 signaling, as the dauer arrest of *daf-2*(e1370) III did not depend on *cep-1* and *daf-2* mutant animals continued to arrest as dauers in a *cep-1* deletion, *cep-1*(gk138) I, background (Supplementary Fig. S6g). Moreover, in agreement with previous reports[69,70], *cep-1* was not required for dauer induction at high temperatures as *cep-1* (gk138) I larvae could enter dauer at 27°C just like wild-type animals (Supplementary Fig. S6h).

The BH3-only proteins *egl-1* and *ced*-13 are known targets of CEP-1/p53 that are upregulated during somatic programmed cell death that occurs during development, and DNA-damage induced germline cell death that occurs in adults upon exposure to ionizing radiation [71-74]. To confirm that CEP-1/p53 was activated in the absence of ILC-17.1, we tested whether these genes were upregulated *ilc-17.1* deleted larvae in a CEP-1/p53 dependent manner. As could be expected, *egl-1* and *ced-13* mRNA levels were upregulated upon CEP-1/p53 overexpression in larvae at both 20°C (Supplementary Fig. S7a) and 25°C (Fig 2f). Both *elg-1* and *ced-13* were also upregulated in *ilc-17.1* deletion mutants, and this upregulation was *cep-1* dependent (Supplementary Fig. S7a; Fig 2f). Chromatin Immunoprecipitation followed by quantitative PCR (ChIP-qPCR) using animals carrying an endogenous CRISPR/Cas9 FLAG tagged *cep*-1 showed that more CEP-1/p53 was bound to the promoter regions of *elg-1* and *ced-13* in larvae lacking *ilc-*

17.1 when compared to wild-type larvae, and the increased occupancy was abrogated when *ilc-17.1* deletion mutants were rescued from dauer arrest by the overexpression of ILC-17.1 in muscle cells (Fig. 2g). These data together confirmed that CEP-1/p53 was activated upon loss of ILC-17.1 signaling, and overexpressing ILC-17.1 in an *ilc-17.1* deletion suppressed this activation.

In mammalian cells, activation of p53 in response to stress increases p53 protein levels through its phosphorylation which allows p53 to escape constitutive degradation mediated by the E3 ubiquitin ligase MDM2[4,5,75]. *C. elegans* genome lacks MDM2 orthologs, but nevertheless CEP-1/p53 has been shown to undergo translational and posttranslational modifications[68,76], although the mechanism of its activation remains incompletely understood. Western analysis of FLAG-tagged endogenous CEP-1/p53 in *C. elegans* showed that CEP-1: FLAG expression was increased in larvae lacking *ilc-17.1*, as seen upon gamma irradiation of animals at doses known to activate CEP-1/p53, and what has been observed in mammalian cells (Fig 2h).

CEP-1/p53 localizes to progenitor blast cells (P cells) in larvae prior to their dauer entry, and directly or indirectly activates a quiescence program.

During *C. elegans* development, most cell divisions are completed during embryogenesis, but a subset of somatic and germline multipotent progenitor or blast cells continue to divide post-embryonically to generate adult tissues such as the gonad, neurons and epidermal cells[77-81]. When larvae arrest as dauers, these cells do not divide, but are maintained in their multipotent state for extended periods of time, and resume division only when larvae continue their postdauer development[77-81]. In the mammalian hematopoietic system, p53 has been shown to be required to maintain stem cells in a quiescent state through its regulation of negative regulators of the cell cycle[82,83]. This is also true of p53 in its role as tumor suppressor, where it restrains cell growth and promotes cell cycle arrest through the transcription of $p21^{WAF1}$ cell cycle inhibitors and other proteins[5,18,19,84]. We therefore reasoned that the activation of CEP-1/p53 that occurred upon loss

of ILC-17.1 signaling that normally signified the presence of food, could serve as a mechanism to link cell cycle control to nutrient availability and protect the organism from developing into an adult when resources were scarce.

In *C. elegans* larvae, CEP-1/p53 has been shown to be expressed in a subset of larval pharyngeal muscle and neuronal cells[65,68]. This has been visualized by others using the same functional, fluorescently tagged CEP-1, CEP-1::GFP which complements the *cep-1* deletion, *cep-1*(*lg12501*), where endogenous CEP-1 protein is not expressed[68]. We found that in addition to these pharyngeal and neuronal cells, in L1 larvae overexpressing CEP-1/p53 and were fated to arrest as dauers, CEP-1/p53 also accumulated in epidermal progenitor blast cells (P cells) (Fig 3a). In *cep-1* (lg12501) I L1 larvae, where *cep-1* is not overexpressed (Supplementary Fig. S6d) and larvae do not arrest as dauers but continue development into reproductive adults (Supplementary Fig. S7b), CEP-1 was also visible in P cells but at significantly lower levels (Fig 3a). These observations suggested that prior to dauer entry, in CEP-1/p53 overexpressing larvae, CEP-1/p53 was active in these progenitor blast cells that would arrest in their multipotent state upon dauer entry.

C. elegans regulates postembryonic cell divisions using over 100 different overlapping and redundant genes[80,85]. Amongst these are the two p21 homologs, *cki-1* and *cki*-2[86,87], and *phg-1,* the *C. elegans* homologue of Gas1 (Growth arrest-specific 1)[86,88-90], a protein that controls cell cycle arrest and quiescence in mammalian cells in response to nutrition (serum) deprivation and harbors p53 consensus binding sites in *C. elegans*. In larvae overexpressing CEP-1/p53 and in larvae lacking *ilc-17.1*, both *cki-1* and *phg-1* were upregulated (Fig. 3b). In addition, *ilc-17.1* deletion mutants displayed increased CEP-1/p53 occupancy at the CEP-1/p53 consensus sites in the *phg-1* gene, although not at the *cki-1* gene, and the increased occupancy was restored to wild-type levels upon ILC-17.1 rescue (Fig 3c; Supplementary Fig. S7c). Thus, CEP-1/p53 activity

329 directly or indirectly upregulated at least two of the several cell cycle inhibitors known to pause
330 cell cycle progression and promote quiescence.
331
332 We asked whether the upregulation of these cell cycle inhibitors was in itself sufficient to trigger
333 dauer arrest. To answer this, we used RNAi to downregulate *cki-1* and *phg-1* and assessed
334 whether this rescued the dauer arrest of *ilc-17.1* deleted larvae and CEP-1/p53 overexpressing
335 larvae and promoted their continuous development. This was partly the case, and downregulating
336 *phg-1* rescued a significant, although small, fraction of *ilc-17.1* deleted and *cep-1* overexpressing
337 larvae from dauer diapause: 6.7± 2.2%, *ilc-17.1* deletion larvae and 10.1 ± 2.2 % *cep-1*
338 overexpressing larvae grew into reproductive adults instead of arresting as dauers on *phg-1* RNAi,
339 compared to 0% and 0.7 ± 0.3% on control RNAi (Fig 3d). RNAi-mediated knockdown of *cki-1*
340 also caused a variable and small fraction of larvae to bypass dauer arrest (Fig 3d). Moreover,
341 larvae that remained phenotypically arrested as dauers even after RNAi-induced knockdown of
342 *phg-1* and *cki-1,* displayed non-dauer traits such as increased rates of sporadic pumping (Fig 3e).
343
344 One of the molecular signatures of quiescence is low metabolic activity, reflected in part by a
345 decrease in the expression of mitochondrial enzymes including cytochrome C[82,83]. RNA-seq data
346 showed that the mRNA expression of the majority of enzymes involved in glycolysis or oxidative
347 phosphorylation (OXPHOS)[91] were not altered in *ilc-17.1* deletion mutants prior to their entry into
348 dauer (Supplementary Figure S8 a-f; Supplementary Table 6). However, the mRNA levels of
349 phosphofructokinase-1.2 (*pfk-1.2*), the key rate limiting enzyme in glycolysis, and
350 cytochrome *c* (*cyc-2.2*), the subunit of complex IV of the electron transport chain responsible for
351 the final transfer of reducing equivalents to O_2, were dramatically decreased in *ilc-17.1* larvae,
352 and in larvae that overexpressed CEP-1/p53 (Supplementary Figure S8 a, d, e). These changes
353 were confirmed by qRT-PCR (Supplementary Figure S8g and Fig 3f). In mammalian cells, p53
354 activity indirectly decreases the expression of enzymes required for glycolysis and indeed, the

355 decrease in mRNA expression of *pfk-1.2* was a downstream consequence of CEP-1/p53
356 activation in the *ilc-17.1* deleted larvae: the deletion of *cep-1* rescued the low mRNA levels
357 (Supplementary Figure S8g). Surprisingly, the decrease in *cyc-2.2* expression was also
358 dependent on CEP-1/p53, but also on DAF-16/FOXO, as the deletion of *cep-1* or *daf-16* rescued
359 the low *cyc-2.2* mRNA levels in *ilc-17.1* deleted larvae (Fig 3f). Moreover, although the
360 downregulation of *pfk-1.2. or cyc-2.2* alone was not sufficient to induce dauer in wild-type animals,
361 RNAi induced downregulation of *cyc-2.2* in *ilc-17.1* deleted larvae increased the percentage of
362 larvae that arrested as dauers under optimal conditions at temperatures of 20°C, suggesting that
363 CEP-1/p53-dependent decrease of *cyc-2.2* was promoting dauer arrest (Supplementary Figure
364 S8h).
365
366 Taken together, these data indicate that the lack of ILC-17 activates CEP-1/p53, which
367 accumulates in larval blast cells, and in addition, directly or indirectly activates a quiescence
368 program, by upregulating the cyclin-dependent kinase inhibitors *cki-1* and the Gas1 ortholog, *phg-*
369 *1*, and the downregulating key metabolic enzymes including Cytochrome C, *cyc-2.2*. These
370 pathways likely collaborate to decrease glucose utilization and trigger the dauer diapause state
371 of larvae, although surprisingly, CEP-1/p53-mediated increase in *cki-1* or *phg-1* was sufficient by
372 itself to promote the dauer decision at a low frequency, and downregulation of Cytochrome C *cyc-*
373 *2.2,* alone in an *ilc-17.1* background was sufficient to increase the fraction of larvae that transiently
374 entered dauer.
375
376 **ILC-17.1 suppresses CEP-1/p53 in *C. elegans* and human epithelial cells.**
377 Since our data pointed towards a model whereby ILC-17.1 signaling that occurred constitutively,
378 under favorable conditions in the presence of food, suppressed CEP-1/p53 to promote continuous
379 development, we directly examined whether IL-17-dependent suppression of CEP-1/p53 activity
380 was a conserved mechanism in mammalian cell culture and in *C. elegans.* Indeed, stimulation of

human epithelial cells with human recombinant IL-17A induced a modest but significant downregulation of p53 expression levels (Fig. 4a). This was similar to the decrease in CEP-1/p53 levels seen in *C. elegans* upon overexpression and paracrine activity of ILC-17.1 (Fig. 2h). For the experiments in mammalian cells, IL-17A stimulation of epithelial cells was confirmed at 18hrs by measurement of secreted CXCL5, a key cytokine downstream of IL-17A signaling[92] (Supplementary Fig. S9a).

In *C. elegans* also increased ILC-17.1 signaling suppressed CEP-1/p53 activation: just as ILC-17.1 overexpression rescued the dauer phenotype of *ilc-17.1* deletion mutants, overexpressing ILC-17.1 also inhibited the dauer arrest of *cep-1* overexpressing animals (Fig. 4b) and inhibited the increase in mRNA levels of CEP-1/p53 target genes, *egl-1* and *ced-13* in animals overexpressing CEP-1/p53 (Fig 2f; Supplementary Fig S7a). In addition, overexpressing ILC-17.1 alone was sufficient to suppress the increased levels of *cki-1* and *phg-1* in *cep-1* overexpressing larvae (Fig. 3b) and restore the decreased *cyc-2.2* mRNA levels that occurred upon CEP-1/p53 overexpression (Fig 3f). In *C. elegans* the activity of CEP-1/p53 has been best studied in adult animals where CEP-1/p53 controls germline apoptosis that occurs in response to genotoxic insults[65,73,86]. Therefore, to examine whether ILC-17.1 could also inhibit the canonical activity of CEP-1/p53, i.e., apoptosis in the adult germline, we subjected wild-type animals, CEP-1/p53 overexpressing animals, and animals overexpressing both CEP-1/p53 and ILC-17.1, to gamma irradiation and measured the number of apoptotic corpses in the germlines of these animals (Fig 4c). As could be expected, CEP-1/p53 overexpression caused an increase in physiological apoptosis that normally occurs during oogenesis in the germline, and in apoptosis that occurs in response to gamma irradiation (Fig 4c). Overexpressing ILC-17.1 in animals that also overexpressed CEP-1/p53, significantly decreased normal as well as irradiation-induced apoptosis (Fig 4c).

Discussion.

Here we show, for the first time, a role for CEP-1/p53 in *C. elegans* development. Our data support a model whereby the IL-17 cytokine ortholog, ILC-17.1, secreted by larval neurons in response to food, links food availability to the developmental decision to grow or enter the quiescent dauer stage by controlling the multifaceted transcriptional program of CEP-1/p53 (Fig. 4d). Specifically, our data show that the CEP-1/p53 needs to be repressed during larval stages to ensure the continuous growth of the animal into reproductive adults, and this repression is mediated by ILC-17.1 signaling through systemically expressed IL-17 receptors. In the absence of ILC-17.1, larvae automatically activate the dauer dormancy decision, and arrest as quiescent dauer larvae, either transiently, or for longer durations. The propensity for dauer arrest appears to be modulated by the extent of CEP-1/p53 activation, which is lower at 20°C compared to 25°C. Dauer arrest is also dependent on the repression of cytochrome C (*cyc-2.2*) levels which, in mammalian systems also maintains stem cell quiescence, directly or indirectly by CEP-1/p53 and DAF-16/FOXO. The site of CEP-1/p53 activity which results in a systemic alteration of the *C. elegans* developmental program needs to be identified; however intriguingly, prior to the dauer decision, in CEP-1/p53 overexpressing animals, CEP-1 expression is upregulated in the P blast cells which remain multipotent until dauer exit.

Nutrient scarcity has shaped much of evolution, and the ability of cells and organisms to sense nutrients and prepare to immediately utilize these resources for growth and development or pause cell cycle progression and maintain a quiescent state until conditions are favorable again, has unquestionable selective advantages. For *C.* elegans, like for most organisms, the availability of food is not guaranteed, and therefore the organism uses different strategies to optimize reproductive success. *C. elegans* larvae develop into reproductive adults when food is plentiful, but enter a stress-resistant, quiescent dauer state adapted for persistence and dispersal when they sense that nutrients are insufficient[25]. Given the growing understanding of the roles of p53 in

regulation of stem cell differentiation and quiescence, it is tempting to speculate that, as seen in *C. elegans*, the p53-family of proteins evolved to link information regarding nutrient availability with the metabolic control of cell cycle progression. Indeed, in mammalian cells, glucose deprivation has been shown to activate p53[93], and p53 is essential for maintaining stem cell quiescence in the hematopoietic system and other organs during steady state tissue homeostasis[82,83].

It is also notable that ILC-17.1 is secreted by *C. elegans* sensory neurons to control CEP-1/p53 activity. Neuronal control of other cell autonomous stress-responsive transcriptional programs such as the cellular response to protein misfolding has been described in *C. elegans* by our group and others, where the nervous system acts to coordinate the transcriptional and epigenetic responses of cells to environmental stress with organismal physiology and behavior[94-97]. In this regard, it is intriguing that the loss of ILC-17.1 signaling in *C. elegans*, which we show decreases Cytochrome C expression levels in a CEP-1/p53-dependent manner, has been shown in previous studies to control the animals' aversive response to oxygen[14]. Thus, it is likely that the metabolic changes triggered by CEP-1/p53 activation and organismal behavior feedback onto each other to influence organismal physiology. In mammals too, resident neurons and immune molecules in peripheral tissue profoundly influence cell fate decisions to remodel tissue architecture during development, organogenesis, inflammatory responses, and in diseases such as cancer[98,99]. It is therefore not far-fetched to imagine that similar neuronal control over p53 and cell quiescence exists in mammalian systems, albeit, perhaps modulated locally through peripheral innervation and immune cells. Such a control mechanism, if it exists, could open new avenues for therapeutic intervention in cancer and other diseases.

The repression of p53 by IL-17 cytokines appears to be conserved between *C. elegans* and human cells and pro-inflammatory cytokines such as the IL-17s are linked to the formation and

proliferation of solid tumors[9,10,100]. However, much needs to be understood before one can directly extrapolate the interaction between *C. elegans* ILC-17.1 and CEP-1/p53 to the mammalian context[4,5,18,19,65]. Importantly, in mammalian systems where cytokines suppress p53, this typically occurs through the activation of Nuclear factor-κB (NF-κB)[101], and the *C. elegans* genome lacks NF-κB[102]. Nevertheless, as in mammals, *C. elegans* development requires the postembryonic division and differentiation of progenitor cell populations that can, under adverse conditions be maintained in a quiescent state. Thus, dissecting the role of p53 in *C. elegans* development to understand how its likely function in blast cells can systemically change the developmental trajectory of the whole organism, could yield far-reaching insights.

Acknowledgements

We thank the V.P. laboratory, Drs. Sarit Smolikove, Josep Comeron and Anna Malkova for comments, Dr. Peter Ratcliffe, Oxford, for his generous gift of *CeHIF-1* antibody, and Dr. Mario Bono, Institute of Science and Technology Austria (ISTA) for *C. elegans* strains not used in this study. Nematode strains were provided by the Caenorhabditis Genetics Center (CGC) (funded by the NIH Infrastructure Programs P40 OD010440). This work was supported by NIH R01 AG060616 (V.P.).

Author Contributions

All authors designed the study, performed experiments, analyzed data, and drafted the manuscript. P.D.I coordinated the mammalian experiments, V.P. coordinated the project. All authors approved the final version of the manuscript.

Declaration of Interests

The authors declare no competing interests

Data Availability

The following data sets were generated

Genes deferentially expressed in the following *C. elegans* larvae bleach-hatched and allowed to grow for 30-34 hrs. at 25°C: wild type (N2), *ilc-17.1*(syb5296) X and praEx022 (*unc-54*p::*ilc-17.1* cDNA::3XFLAG::*tbb-2* 3'UTR; p*dat-1*::GFP::*unc-54* 3'UTR).

The data discussed in this publication have been deposited in NCBI's Gene Expression Omnibus (Edgar et al., 2002) and are accessible through GEO Series accession number GSE218596, https://www.ncbi.nlm.nih.gov/geo/query/acc.cgi?acc=GSE218596

Figure 1

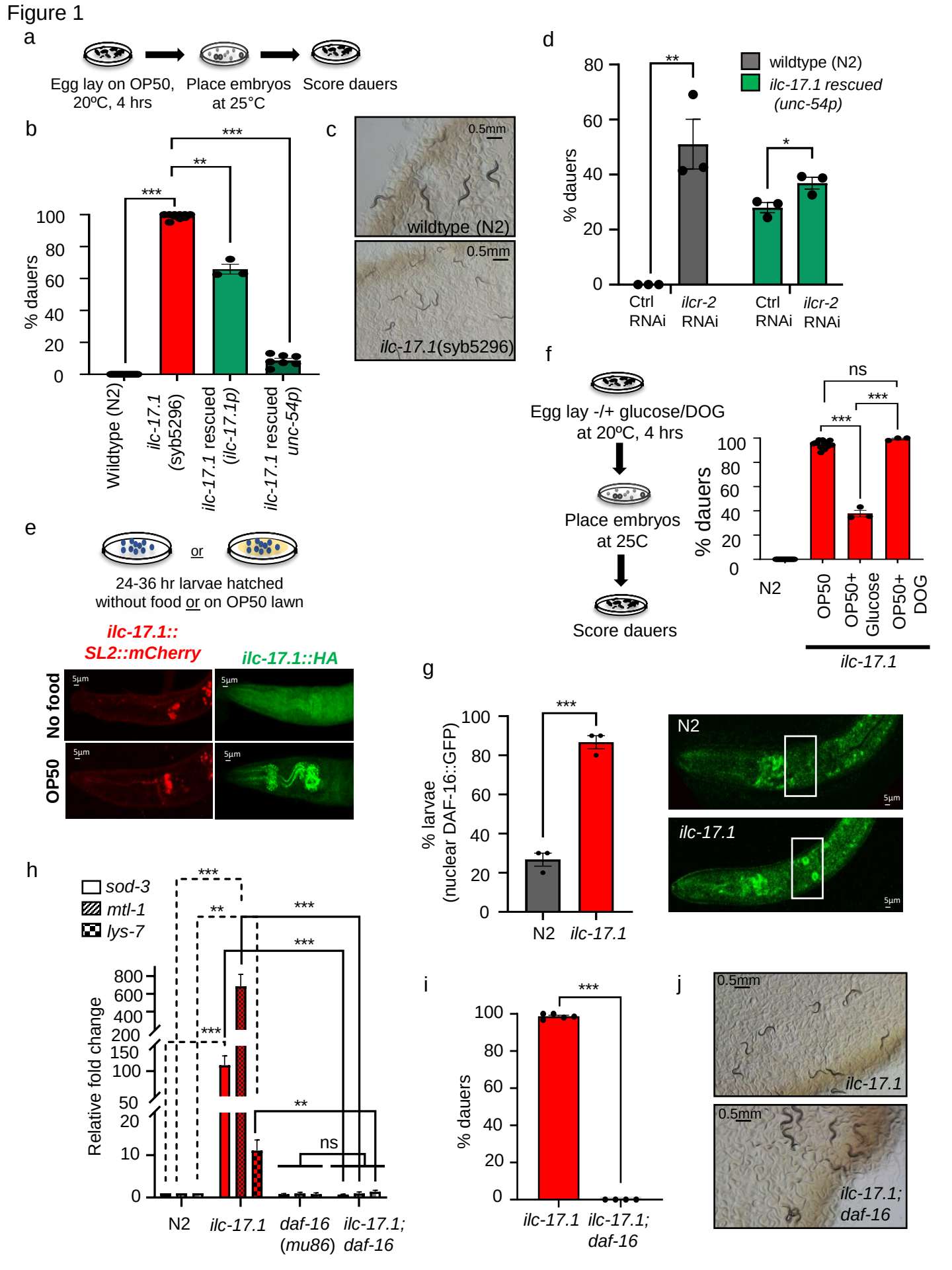
a
Egg lay on OP50, 20ºC, 4 hrs
Place embryos at 25°C
Score dauers
b
% dauers
Wildtype (N2)
ilc-17.1 (syb5296)
ilc-17.1 rescued (ilc-17.1p)
ilc-17.1 rescued unc-54p)
c
0.5mm
wildtype (N2)
ilc-17.1(syb5296)
d
wildtype (N2)
ilc-17.1 rescued (unc-54p)
% dauers
Ctrl RNAi
ilcr-2 RNAi
e
or
24-36 hr larvae hatched without food or on OP50 lawn
ilc-17.1:: SL2::mCherry
ilc-17.1::HA
No food
OP50
f
Egg lay -/+ glucose/DOG at 20ºC, 4 hrs
Place embryos at 25C
Score dauers
% dauers
N2
OP50
OP50+ Glucose
OP50+ DOG
ilc-17.1
g
% larvae (nuclear DAF-16::GFP)
N2
ilc-17.1
h
sod-3
mtl-1
lys-7
Relative fold change
N2
ilc-17.1
daf-16 (mu86)
ilc-17.1; daf-16
i
% dauers
ilc-17.1
ilc-17.1; daf-16
j
0.5mm
ilc-17.1
ilc-17.1; daf-16

Figure 1: ILC-17.1 secreted by larval neurons in response to food availability is required to prevent dauer arrest.

a. Schematic of experiment to assess dauer arrest. Note: embryos were laid for 4 hours by day-one gravid adults under optimal growth conditions: on OP50 lawns, and at 20°C. Adults were subsequently removed and embryos were moved to 25°C. Unless otherwise mentioned, in these and subsequent experiments, all dauer assays were conducted at 25°C, and dauers were scored 48-72 hours after egg lay.

b. Percentage of larvae that arrest as dauers. *n*=3-7 experiments. ***$p < 0.001$, **$p < 0.01$. (analysis of variance (ANOVA) with Tukey's correction).

c. Representative micrographs. **Top:** Wildtype (N2) grew to L4s. **Bottom:** *ilc-17.1*(syb5296) X larvae arrested as dauers. Scale bar, 0.5mm

d. Percentage of wildtype (N2) and *ilc-17.1*(syb5296) X larvae that arrest as dauers on control (L4440; Ctrl) and *ilcr-2* RNAi. **$p < 0.01$, *$p < 0.05$ (analysis of variance (ANOVA) with Tukey's correction). *n*=3 experiments.

e. Top: Schematic of experiment to assess localization of *ilc-17.1* mRNA and ILC-17.1 protein in the presence (OP50) and absence of food. Embryos hatched at 20°C and imaged after 24-36 hours (L1 stage larvae). **Bottom:** Representative micrographs showing projections of confocal z-sections of pharyngeal region of 24-36 hr. larvae. **left:** mCherry co-expressed with *ilc-17.1* mRNA is in amphid neurons. **right**: projection of z-sections showing immunostaining with anti-HA antibody to visualize CRISPR tagged endogenous ILC-17.1::HA in larvae. Scale bar, 5µm.

f. **Left**: Schematic of experimental design. **Right**: Percent dauers: wildtype (N2) and *ilc-17.1*(syb5296) X larvae on OP50 alone, and on OP50 + 50mM glucose or 50mM DOG. *n*=3-13 experiments. ***p < 0.001, (analysis of variance (ANOVA) with Tukey's correction).

g. **Left**: Percent larvae where DAF-16::GFP was localized in the intestinal nucleus. Larvae were grown at 20°C larvae for 36 hr**.** *n*=3 experiments. ***p < 0.001. (unpaired t-test). Note: experiments were conducted at 20°C, since at 25°C, DAF-16::GFP was constitutively in the intestinal nuclei even in wildtype larvae. **Right:** representative micrographs showing DAF-16::GFP localization in wildtype and *ilc-17.1*(syb5296) X larvae. Scale bar, 5µm

h. Average *sod-3, mtl-1, and lys-7* mRNA levels in 30-36 hr. old larvae grown at 25°C. mRNA levels were determined relative to *pmp-3* and normalized to that in wildtype (N2). *n*=4-10 experiments. ***p < 0.001, **p < 0.01, ns=not significant, (unpaired t-test).

i. Percent dauers upon deleting *daf-16* in *ilc-17.1* mutants. *n*=3-5 experiments. ***p < 0.001, (unpaired t-test).

j. Representative micrographs. *ilc-17.1*(syb5296) X larvae arrested as dauers but *ilc-17.1* deleted larvae grew into L4s and reproductive adults in a *daf-16* deficient background, i.e. *daf-16(mu86).* Scale bar:0.5mm

Data in all graphs show mean ± s.e.m.

Figure 2

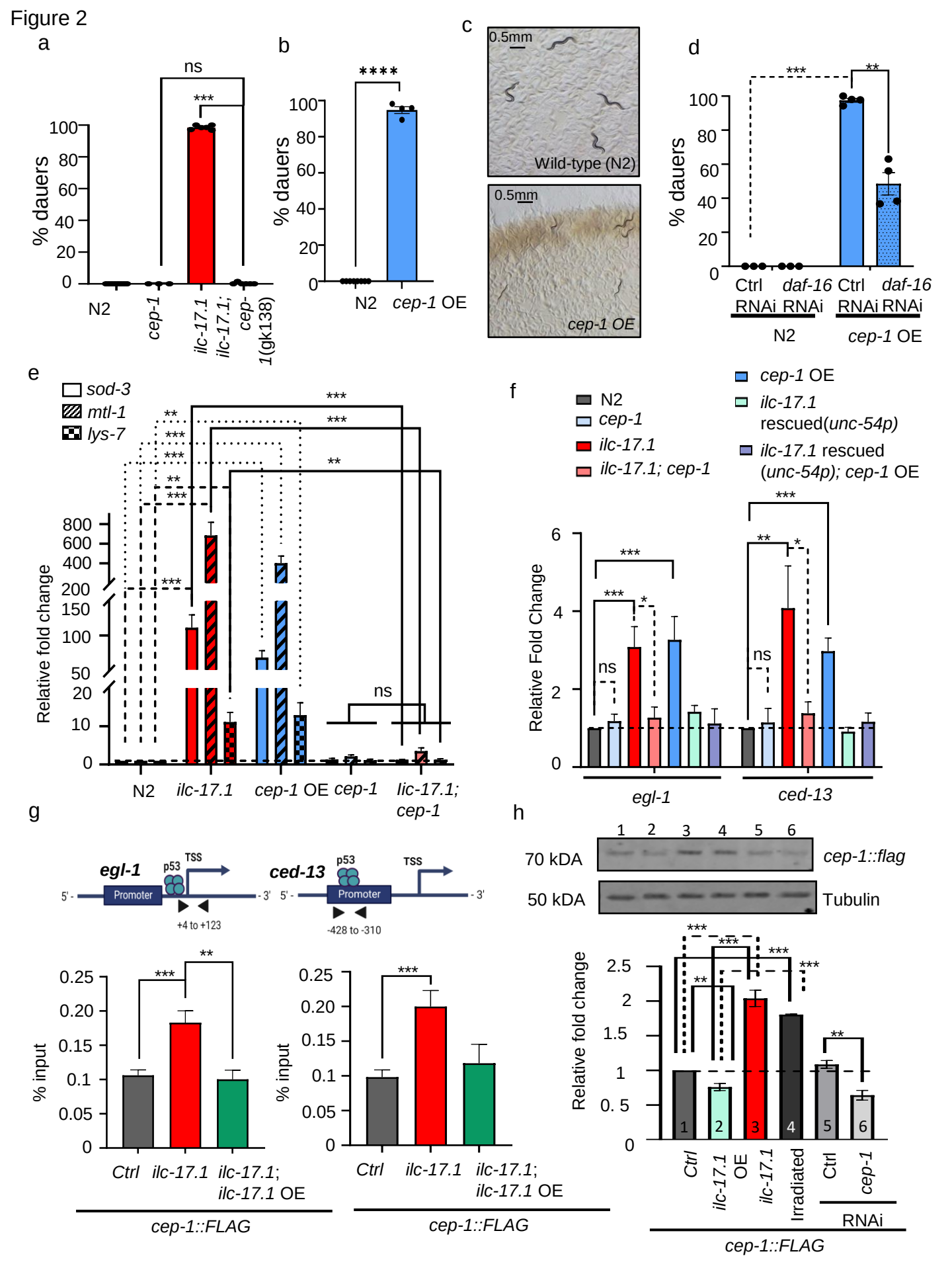
a
ns
***
% dauers
N2
cep-1
ilc-17.1
ilc-17.1; cep-1(gk138)
b
****
% dauers
N2
cep-1 OE
c
0.5mm
Wild-type (N2)
0.5mm
cep-1 OE
d
***
**
% dauers
Ctrl RNAi
daf-16 RNAi
Ctrl RNAi
daf-16 RNAi
N2
cep-1 OE
e
sod-3
mtl-1
lys-7
Relative fold change
N2
ilc-17.1
cep-1 OE
cep-1
ilc-17.1; cep-1
ns
f
N2
cep-1
ilc-17.1
ilc-17.1; cep-1
cep-1 OE
ilc-17.1 rescued(unc-54p)
ilc-17.1 rescued (unc-54p); cep-1 OE
Relative Fold Change
egl-1
ced-13
g
egl-1
ced-13
p53
TSS
Promoter
5'
3'
+4 to +123
-428 to -310
% input
Ctrl
ilc-17.1
ilc-17.1; ilc-17.1 OE
cep-1::FLAG
h
1 2 3 4 5 6
70 kDA
cep-1::flag
50 kDA
Tubulin
Relative fold change
Ctrl
ilc-17.1 OE
ilc-17.1 Irradiated
Ctrl
cep-1
RNAi
cep-1::FLAG

Figure 2: IL-17 modulates CEP-1/p53 activity to control dauer arrest.

a. Percent dauers. *n*=3-8 experiments. ***p < 0.001, ns, not significant, (analysis of variance (ANOVA) with Tukey's correction).

b. Percent dauers. *n*=4 experiments. ***p < 0.001, (analysis of variance (ANOVA) with Tukey's correction).

c. Representative micrographs. **Top:** Wildtype (N2) grew to L4s. **Bottom:** *cep-1* overexpressing larvae arrested as dauers. Scale bar:0.5mm.

d. Percent wildtype (N2) and *cep-1* overexpressing larvae that arrest as dauers on control and *daf-16* RNAi. *n*=4 experiments. ***p < 0.001, **p < 0.01 (analysis of variance (ANOVA) with Tukey's correction).

e. Average *sod-3, mtl-1, and lys-7* mRNA levels in 30-36 hr. old larvae grown at 25°C. mRNA levels were determined relative to *pmp-3* and normalized to that in wildtype (N2). *n*=6-10 experiments. ***p < 0.001, **p < 0.01. (unpaired t-test).

f. Average *egl-1* and *ced-13* mRNA levels in 30-36 hr. larvae grown at 25°C. mRNA levels were determined relative to *pmp-3* and normalized to that in wildtype (N2). *n*=6-7 experiments. ***p < 0.001, **p < 0.01, *p < 0.05, ns=not significant, (unpaired t-test).

g. CEP-1 occupancy (expressed as percent input) in 30-36 hr. larvae grown at 25°C, measured at the promoter proximal regions of *egl-1* and *ced-13* (Top schematic). CEP-1 occupancy was assayed in animals where endogenous *cep-1* was FLAG tagged at its C-terminus using CRISPR/Cas9, and immunoprecipitated with anti-FLAG antibody. Stains

used: CEP-1::FLAG expressing animals in control wild-type background (Ctrl), in *ilc-17.1*(syb5296) X background, and in *ilc-17.1*(syb5296)X rescued from dauer arrest by overexpressing ILC-17.1 under the *unc-54* promoter (*ilc-17.1; ilc-17.1* OE). *n*=4 experiments. ***p < 0.001, **p < 0.01. (unpaired t-test).

h. **Top**: Representative Western blot showing CEP-1: FLAG and tubulin when crossed into *ilc-17.1* overexpressing and deletion backgrounds. *cep-1* RNAi serves to show specificity. **Bottom**: CEP-1 levels were quantified relative to tubulin and normalized to control animals (CEP-1::FLAG in wildtype background). *n*=4 experiments. Numbers in data bars correspond to representative bands on western. ***p < 0.001, **p < 0.01 (unpaired t-test).

Data in all graphs show mean ± s.e.m.

Figure 3

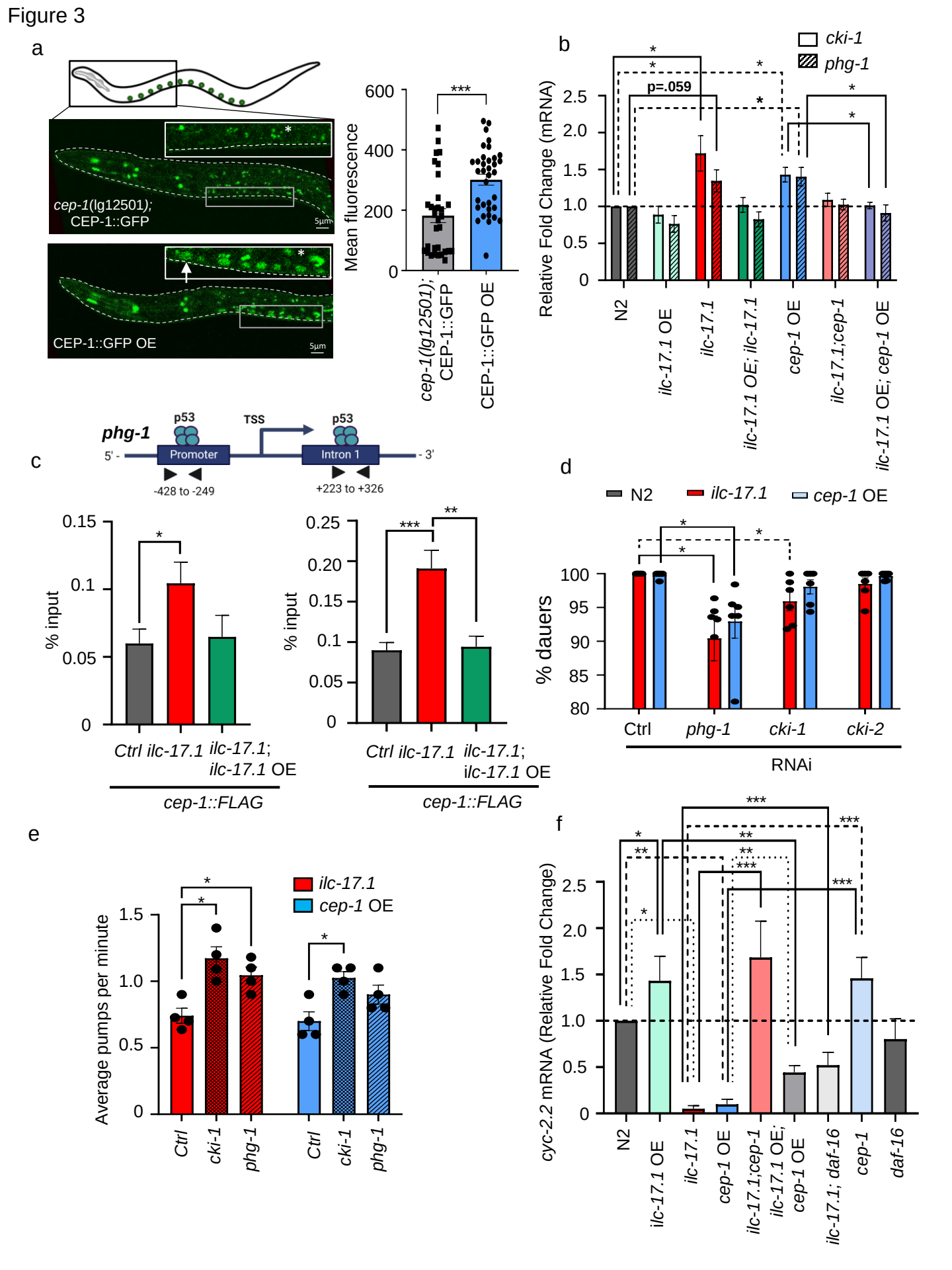
a
cep-1(lg12501); CEP-1::GFP
CEP-1::GFP OE
5µm
Mean fluorescence
600
400
200
0
***
cep-1(lg12501); CEP-1::GFP
CEP-1::GFP OE
b
cki-1
phg-1
Relative Fold Change (mRNA)
p=.059
N2
ilc-17.1 OE
ilc-17.1
ilc-17.1 OE; ilc-17.1
cep-1 OE
ilc-17.1;cep-1
ilc-17.1 OE; cep-1 OE
c
phg-1
p53
TSS
Promoter
Intron 1
5' -
- 3'
-428 to -249
+223 to +326
% input
Ctrl
ilc-17.1
ilc-17.1; ilc-17.1 OE
cep-1::FLAG
d
N2
ilc-17.1
cep-1 OE
% dauers
Ctrl
phg-1
cki-1
cki-2
RNAi
e
ilc-17.1
cep-1 OE
Average pumps per minute
Ctrl
cki-1
phg-1
f
cyc-2.2 mRNA (Relative Fold Change)
N2
ilc-17.1 OE
ilc-17.1
cep-1 OE
ilc-17.1;cep-1
ilc-17.1 OE; cep-1 OE
ilc-17.1; daf-16
cep-1
daf-16

Figure 3: Active CEP-1/p53 is expressed in multipotent progenitor cells (P cells) prior to dauer arrest and upregulates cell cycle inhibitors and downregulates metabolic enzymes.

a. **Left:** Representative micrographs of anterior region of 15-20 hr. L1 larvae at 25°C, showing CEP-1::GFP expression in the ventral surface postembryonic blast cells (P blast cells; arrow). Gut granule background fluorescence indicated with asterix. A schematic is shown above. Insets: zoom-in on the P blast cells. **Right:** CEP-1::GFP expression in P cells of CEP-1 overexpressing larvae and in larvae harboring a deletion (*lg12501*) in the endogenous *cep-1* gene. *n*=3 experiments. ***p < 0.001, (unpaired t-test). For *cep-1* mRNA expression levels see **Supplementary Fig. S6d**.

b. Average *cki-1* and *phg-1* mRNA levels in 30-36 hr. larvae grown at 25°C. mRNA levels were determined relative to *pmp-3* and normalized to that in wildtype (N2). *n*=4-6 experiments. *p < 0.05. (unpaired t-test).

c. CEP-1 occupancy (expressed as percent input) in 30-36 hr. larvae grown at 25°C, measured at the promoter proximal region, and in the first intron of *phg-1* (Schematic on top). CEP-1 occupancy was assayed in animals where endogenous *cep-1* was FLAG tagged at its C-terminus using CRISPR/Cas9, and immunoprecipitated with anti-FLAG antibody. Stains used: CEP-1::FLAG expressing animals in control wild-type background (Ctrl), in *ilc-17.1*(syb5296) X background, and in *ilc-17.1*(syb5296)X rescued from dauer arrest by overexpressing ILC-17.1 under the *unc-54* promoter (*ilc-17.1; ilc-17.1* OE). *n*=4 experiments. ***p < 0.001, **p < 0.01, *p < 0.05. (unpaired t-test).

d. Percent dauers in *ilc-17.1* larvae and *cep-1* overexpressing larvae upon RNAi induced downregulation of *cki-1* and *phg-1. n*=6 experiments. *p < 0.05, (analysis of variance (ANOVA) with Tukey's correction).

603

604 **e.** Average pumps/minute in *ilc-17.1* and *cep-1* dauers when subjected to control (L4440; Ctrl),
605 *cki-1* and *phg-1* RNAi. *n*= 4 experiments, and 10 dauers were scored per experiment. *p < 0.05
606 (unpaired t-test).

607

608 **f.** Average *cyc-2.2* mRNA levels in 30-36 hr. larvae grown at 25°C. mRNA levels were
609 determined relative to *pmp-3* and normalized to that in wildtype (N2). *n*=4-6 experiments.
610 ***p < 0.001, **p < 0.01, *p < 0.05. (unpaired t-test).

611

612 Data in all graphs show mean ± s.e.m.

Figure 4

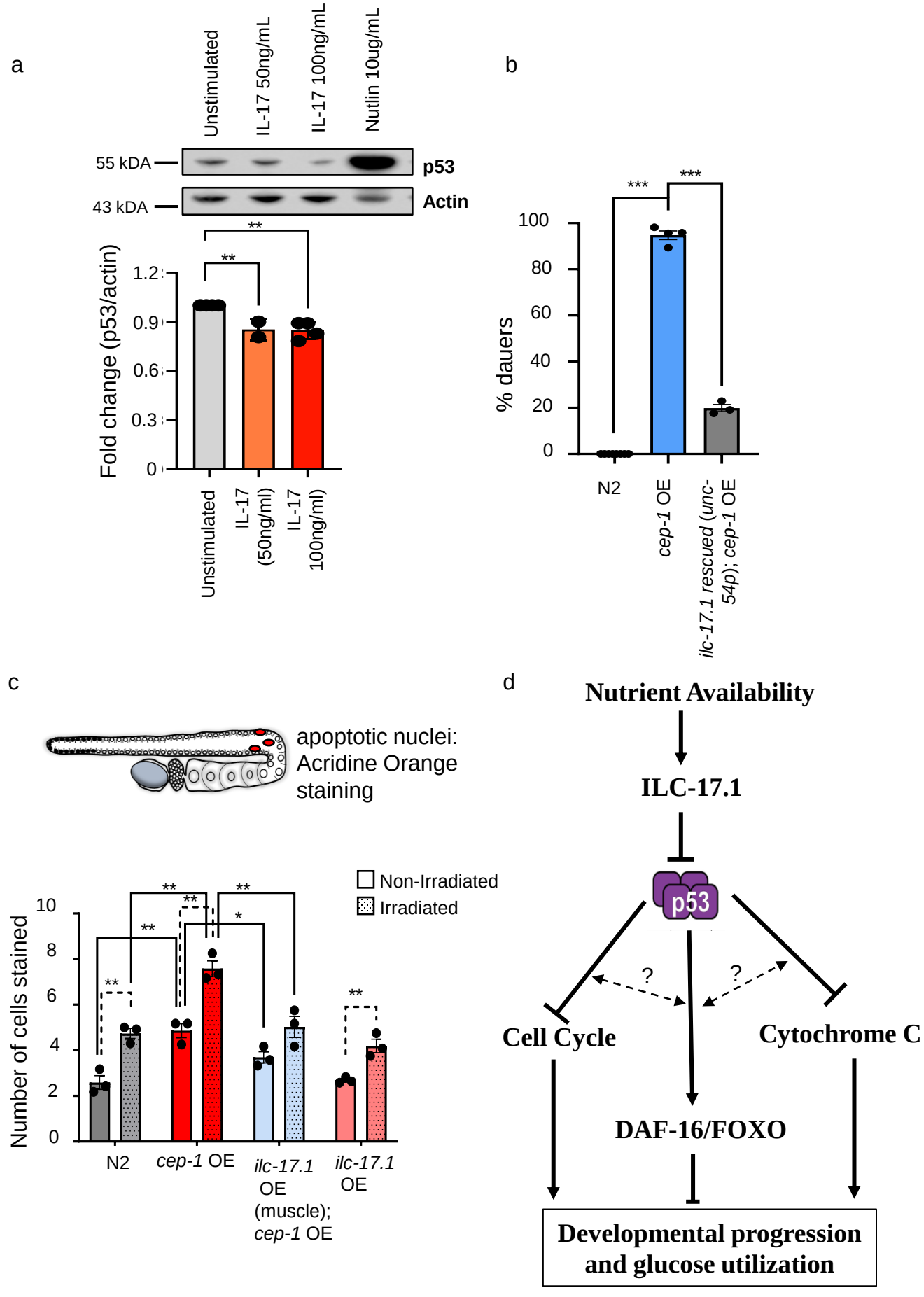
a
Unstimulated
IL-17 50ng/mL
IL-17 100ng/mL
Nutlin 10ug/mL
55 kDA
p53
43 kDA
Actin
Fold change (p53/actin)
1.2
0.9
0.6
0.3
0
Unstimulated
IL-17 (50ng/ml)
IL-17 100ng/ml
b
% dauers
100
80
60
40
20
0
N2
cep-1 OE
ilc-17.1 rescued (unc-54p); cep-1 OE
c
apoptotic nuclei: Acridine Orange staining
Non-Irradiated
Irradiated
Number of cells stained
10
8
6
4
2
0
N2
cep-1 OE
ilc-17.1 OE (muscle); cep-1 OE
ilc-17.1 OE
d
Nutrient Availability
ILC-17.1
p53
?
?
Cell Cycle
Cytochrome C
DAF-16/FOXO
Developmental progression and glucose utilization

Figure 4: ILC-17.1 suppresses CEP-1/p53 in *C. elegans* and mammalian epithelial cells.

a. **Top:** Representative Western blot showing p53 levels in A459 epithelial cells stimulated for 18hrs with increasing doses of rIL-17. β-actin was used as a loading control and Nutlin was used as a positive control. **Bottom:** Quantification of p53 levels normalized to actin levels. *n*= 2-4 independent experiments. **p<0.01, (One-Way ANOVA with uncorrected Fisher's LSD).

b. Percent dauers upon overexpressing ILC-17.1 (ectopic expression under the muscle specific *unc-54* promoter) in *cep-1* overexpressing larvae at 25°C. *n*=4 experiments. ***p < 0.001, (analysis of variance (ANOVA) with Tukey's correction).

c. **Top:** Schematic of germline apoptosis (apoptotic cells in red) scored with Acridine Orange. **Bottom:** Average numbers of apoptotic cells in day-one adult animals under control, non-irradiated conditions, and upon irradiation with 75 Gy. *n*= 3 experiments, and 12 gonad arms /experiment. **p < 0.01, *p < 0.05 (analysis of variance (ANOVA) with Tukey's correction).

d. Working model showing how the IL-17 cytokine ortholog, ILC-17.1, secreted by larval neurons in response to nutrient availability, suppresses CEP-1/p53 and promotes the developmental decision to continue reproductive growth and glucose utilization; In the absence of ILC-17.1 or excess CEP-1/p53, larvae enter the quiescent dauer stage by activating the different programs of CEP-1/p53.

Data in all graphs show mean ± s.e.m.

Figure S1

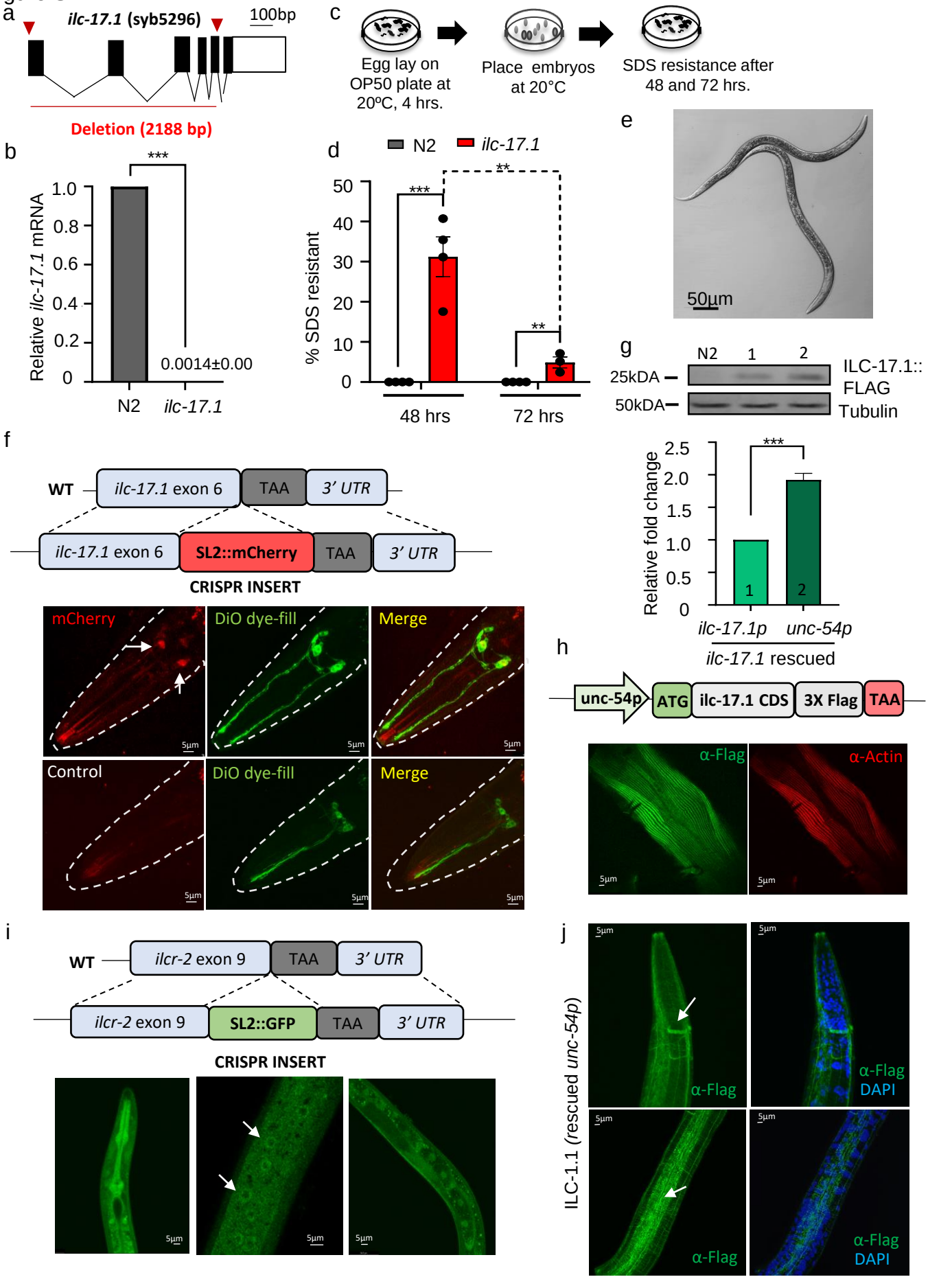
a
ilc-17.1 (syb5296)
100bp
Deletion (2188 bp)
b
***
Relative ilc-17.1 mRNA
1.0
0.8
0.6
0.4
0.2
0
0.0014±0.00
N2
ilc-17.1
c
Egg lay on OP50 plate at 20ºC, 4 hrs.
Place embryos at 20°C
SDS resistance after 48 and 72 hrs.
d
N2
ilc-17.1
% SDS resistant
50
40
30
20
10
0
***
**
**
48 hrs
72 hrs
e
50µm
g
N2
1
2
25kDA
50kDA
ILC-17.1::FLAG
Tubulin
f
WT
ilc-17.1 exon 6
TAA
3' UTR
ilc-17.1 exon 6
SL2::mCherry
TAA
3' UTR
CRISPR INSERT
mCherry
DiO dye-fill
Merge
Control
DiO dye-fill
Merge
5µm
Relative fold change
2.5
2.0
1.5
1.0
0.5
0
***
1
2
ilc-17.1p
unc-54p
ilc-17.1 rescued
h
unc-54p
ATG
ilc-17.1 CDS
3X Flag
TAA
α-Flag
α-Actin
5µm
i
WT
ilcr-2 exon 9
TAA
3' UTR
ilcr-2 exon 9
SL2::GFP
TAA
3' UTR
CRISPR INSERT
5µm
j
ILC-1.1 (rescued unc-54p)
α-Flag
α-Flag
DAPI
α-Flag
α-Flag
DAPI
5µm

Supplementary Figure S1: ILC-17.1 is expressed in amphid neurons and secreted to modulate *C. elegans* developmental diapause.

a. Schematic of *ilc-17.1* gene depicting the syb5296 deletion.

b. Average mRNA expression in *ilc-17.1* (syb5296) X deletion mutants relative to wildtype (N2). *n*=4 experiments. ***p < 0.001, (unpaired t-test).

c. Schematic of experiment leveraging the dauer-resistance to 1% SDS, to determine the percentage of larvae that enter a dauer state during development under optimal conditions at 20°C.

d. Percent of wildtype (N2) and *ilc-17.1* (syb5296) X deletion mutant larvae that transiently enter dauer during development at 20°C. *n*=4 experiments. ***p < 0.001, **p < 0.01, (analysis of variance (ANOVA) with Tukey's correction).

e. Representative micrograph showing DIC image of *ilc-17.1* (syb5296) X deletion mutant dauer larvae, 72 hrs. post-hatching at 25°C. Scale bar=50µm.

f. **Top:** Schematic of CRISPR insertion of SL2: mCherry into *ilc-17.1* locus. **Bottom, upper panel:** Representative micrographs showing mCherry expression in amphid neurons of *C. elegans* expressing mCherry as a bicistronic SL2 cassette along with the endogenous *ilc-17.1* gene to report on sites of *ilc-17.1* mRNA expression. Amphid neurons were identified by DiO dye filling (GFP); mCherry overlapped with a subset of DiO filled neurons. **Bottom, lower panel:** Wildtype (N2; Control) not expressing mCherry imaged to show specificity of mCherry expression. Scale bar=5µm.

g. **Top:** Representative Western blot showing (upper panel) expression of ILC-17.1::FLAG rescue constructs under the *ilc-17.1* promoter (1) and under the *unc-54* promoter (2). Wildtype (N2) were used to show specificity of α-FLAG antibody. (lower panel) tubulin. **Bottom:** ILC-17.1::FLAG expression, quantified relative to tubulin levels and normalized to FLAG levels in animals expressing ILC-17.1::FLAG rescue construct under the *ilc-17.1* promoter (1). *n*=3 experiments. ***p < 0.001 (unpaired t-test).

h. **Top:** Schematic of ILC-17. 1: FLAG rescue contrast driven by the *unc-54* promoter that was overexpressed in *ilc-17.1* (syb5296) X deletion mutants and rescued their dauer arrest. **Bottom:** Representative micrographs showing a z-section of ILC-17. 1: FLAG expressing animals immunostained with α-FLAG antibody, and α-actin (to show expression in body wall muscle cells). Scale bar=5µm

i. **Top:** Schematic of CRISPR insertion of SL2: GFP into *ilcr-2* locus to identify sites of *ilcr-2* expression. **Bottom:** Representative micrographs showing GFP expression in cells of the pharynx (left), epidermal cells (middle; arrows) and gonad (right). Scale bar=5µm

j. Representative micrographs showing two z-sections through animals overexpressing ILC-17.1::FLAG in their body wall muscle cells as in h. Note: ILC-17.1::FLAG is detected at the amphid commissures near the pharynx (top pane; arrow) and in the epidermis (bottom panel; arrows) in addition to the body wall muscle cells (h), Scale bar=5µm

Data in all graphs show mean ± s.e.m.

Figure S2

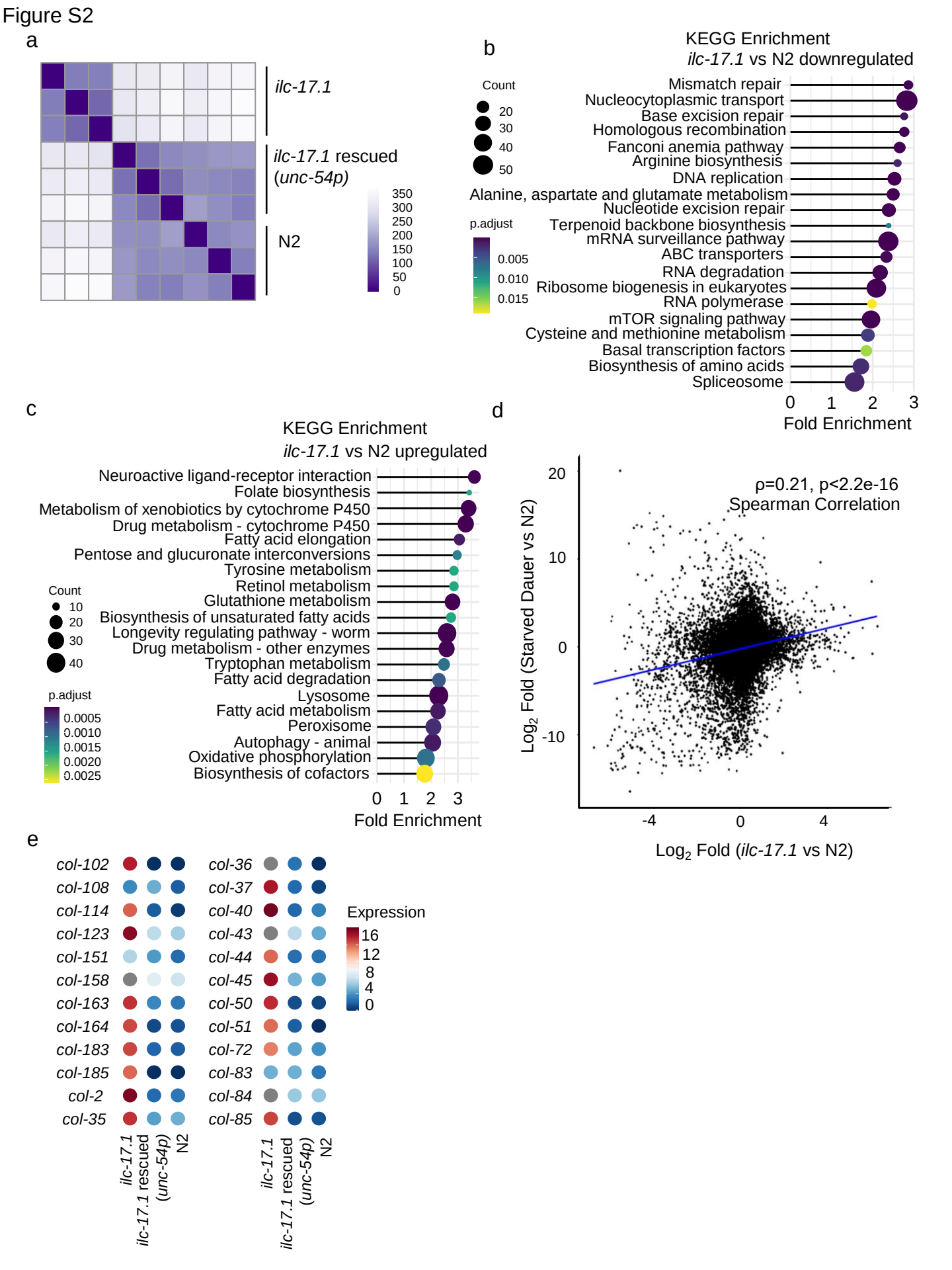
a
ilc-17.1
ilc-17.1 rescued (unc-54p)
N2
350
300
250
200
150
100
50
0
b
KEGG Enrichment
ilc-17.1 vs N2 downregulated
Count
20
30
40
50
p.adjust
0.005
0.010
0.015
Mismatch repair
Nucleocytoplasmic transport
Base excision repair
Homologous recombination
Fanconi anemia pathway
Arginine biosynthesis
DNA replication
Alanine, aspartate and glutamate metabolism
Nucleotide excision repair
Terpenoid backbone biosynthesis
mRNA surveillance pathway
ABC transporters
RNA degradation
Ribosome biogenesis in eukaryotes
RNA polymerase
mTOR signaling pathway
Cysteine and methionine metabolism
Basal transcription factors
Biosynthesis of amino acids
Spliceosome
0 1 2 3
Fold Enrichment
c
KEGG Enrichment
ilc-17.1 vs N2 upregulated
Count
10
20
30
40
p.adjust
0.0005
0.0010
0.0015
0.0020
0.0025
Neuroactive ligand-receptor interaction
Folate biosynthesis
Metabolism of xenobiotics by cytochrome P450
Drug metabolism - cytochrome P450
Fatty acid elongation
Pentose and glucuronate interconversions
Tyrosine metabolism
Retinol metabolism
Glutathione metabolism
Biosynthesis of unsaturated fatty acids
Longevity regulating pathway - worm
Drug metabolism - other enzymes
Tryptophan metabolism
Fatty acid degradation
Lysosome
Fatty acid metabolism
Peroxisome
Autophagy - animal
Oxidative phosphorylation
Biosynthesis of cofactors
0 1 2 3
Fold Enrichment
d
ρ=0.21, p<2.2e-16
Spearman Correlation
Log2 Fold (Starved Dauer vs N2)
20
10
0
-10
-4
0
4
Log2 Fold (ilc-17.1 vs N2)
e
col-102
col-108
col-114
col-123
col-151
col-158
col-163
col-164
col-183
col-185
col-2
col-35
col-36
col-37
col-40
col-43
col-44
col-45
col-50
col-51
col-72
col-83
col-84
col-85
Expression
16
12
8
4
0
ilc-17.1
ilc-17.1 rescued (unc-54p)
N2
ilc-17.1
ilc-17.1 rescued (unc-54p)
N2

Supplementary Figure S2: RNA-seq analysis of ILC-17.1 deficient larvae.

a. Pair-wise distance matrix of RNA-seq samples shows the expected clustering of total RNA of the biological triplicates of each strain. RNA-seq analysis was conducted on total RNA purified from wildtype (N2), *ilc-17.*1 deletion larvae, and *ilc-17.1* deleted larvae overexpressing ILC-17.1 in the body wall muscle cells [*ilc-17.1*rescued *(unc-54*p*)*]. All larvae were grown for 34-36 hrs. at 25°C; wild-type and rescue strains were in late L2, L3 and *ilc-17.1* larvae had not yet arrested as dauers.

b. KEGG enrichments (padust <0.015) associated with significantly (padjust <0.05) differentially downregulated genes.

c. KEGG enrichments (padust <0.0025) associated with significantly (padjust <0.05) differentially upregulated genes.

d. Spearman correlation between all genes in a microarray analysis of dauer larvae that were induced by starvation and *ilc-17.*1 deletion larvae grown for 34-36 hrs. at 25°C. ***p < 0.001.

e. Heatmap depicting expression levels (log_2 normalized counts) of the major dauer-specific collagens in the *ilc-17.1* (syb5296) X deletion mutants, *ilc-17.1* (syb5296) X deletion mutants rescued by the overexpression of ILC-17.1::FLAG in the body wall muscle and wildtype (N2).

Figure S3

a

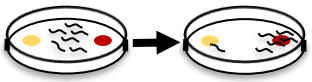

Day-one adults placed at center of plate
and control and odor at opposite ends.
Chemotaxis index, after 1 hour

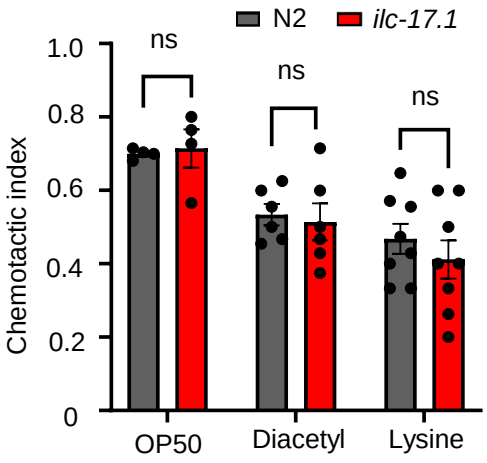

b

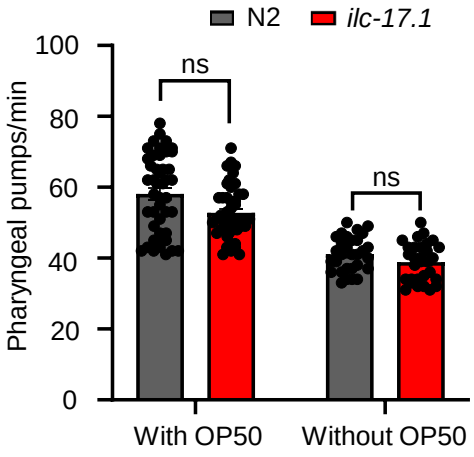

c

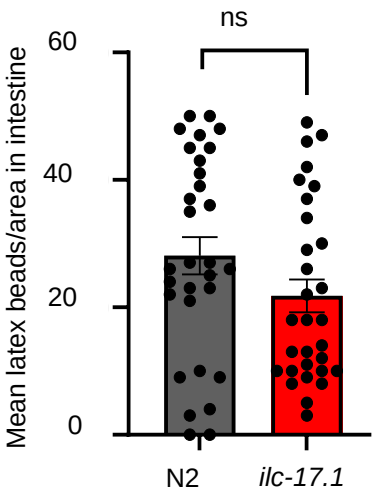

Supplementary Figure S3: Lack of ILC-17.1 does not affect the animals' sensory perception of food.

a. Chemotaxis index towards OP50, 0.01% v/v diacetyl, and 1M lysine for *ilc-17.1* (syb5296) X deletion mutants and wildtype (N2) day-one adults at 20°C. *n*= 5-8 experiments. ns, not significant (unpaired t-test).

b. Number of pharyngeal pumps/min in *ilc-17.1* (syb5296) X deletion mutants and wildtype (N2) day-one adults at 20°C, on OP50 lawns, and on plates without food. *n*= 3 experiments, with at least 5 animals/experiment scored. The pumping rates of individual animals is depicted. ns, not significant (unpaired t-test).

c. Average numbers of fluorescent latex beads in similar areas of distal gut lumen of 40-hour *ilc-17.1* (syb5296) X deletion mutant and wildtype (N2) larvae at 20°C. *n*= 3 experiments, with at 10 animals/experiment. The numbers of beads in individual animals is depicted. ns, not significant (unpaired t-test).

Data in all graphs show mean ± s.e.m.

Figure S4

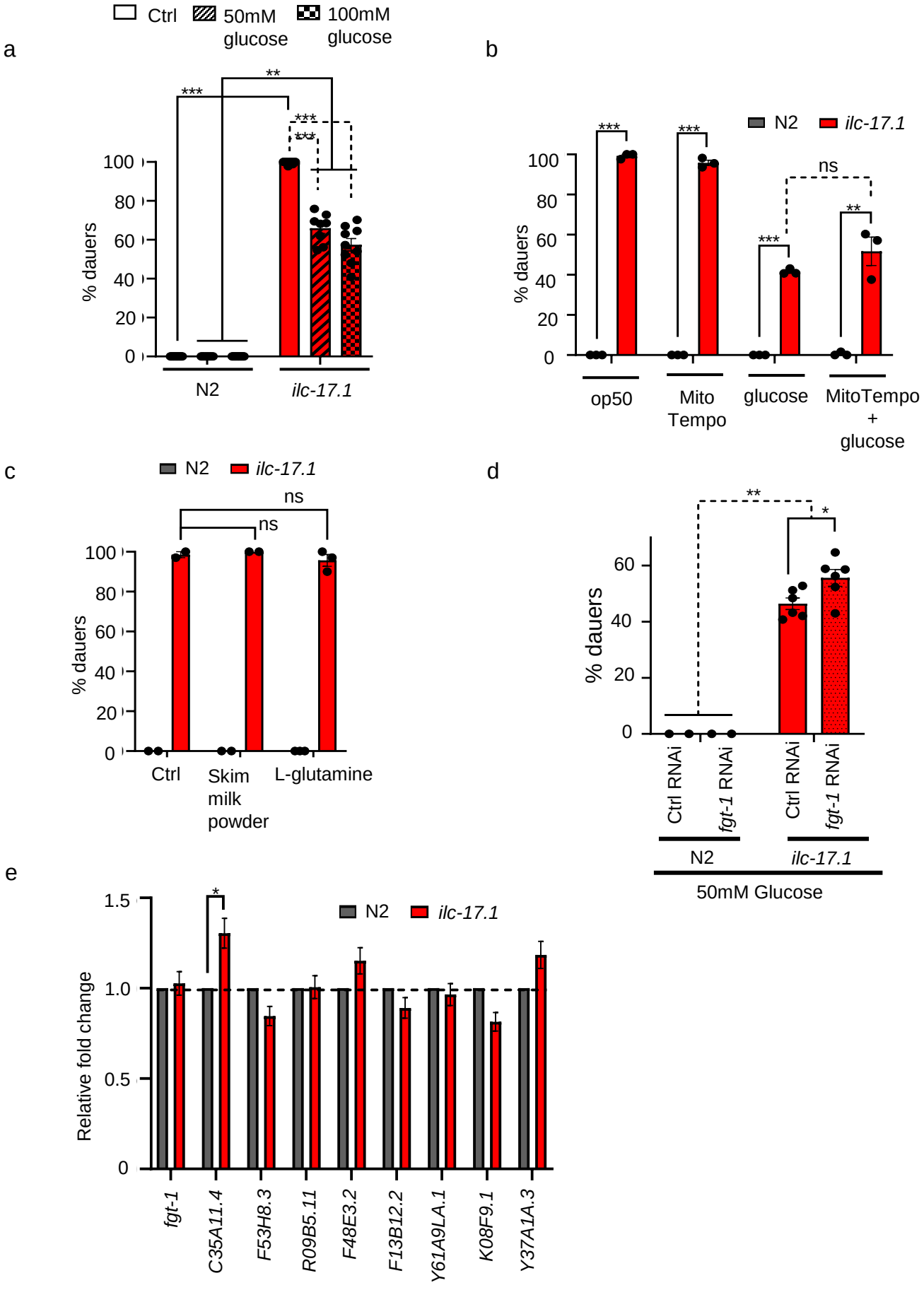
a
Ctrl
50mM glucose
100mM glucose
% dauers
N2
ilc-17.1
b
N2
ilc-17.1
% dauers
op50
Mito Tempo
glucose
MitoTempo + glucose
ns
c
N2
ilc-17.1
% dauers
Ctrl
Skim milk powder
L-glutamine
ns
d
% dauers
Ctrl RNAi
fgt-1 RNAi
N2
ilc-17.1
50mM Glucose
e
N2
ilc-17.1
Relative fold change
fgt-1
C35A11.4
F53H8.3
R09B5.11
F48E3.2
F13B12.2
Y61A9LA.1
K08F9.1
Y37A1A.3

Supplementary Figure S4: ILC-17.1 deficiency inhibits glucose utilization.

a. Percent dauers amongst *ilc-17.1* (syb5296) X deletion mutants and wildtype (N2) larvae on 50mM and 100 mM glucose at 25°C. *n*= 5-9 experiments. ***p < 0.001, **p < 0.01, (analysis of variance (ANOVA) with Tukey's correction).

b. Percent dauers amongst *ilc-17.1* (syb5296) X deletion mutants and wildtype (N2) larvae on 50mM glucose upon exposure to 0.1mM MitoTEMPO at 25°C. *n*= 3 experiments ***p < 0.001, **p < 0.01, ns, not significant, (analysis of variance (ANOVA) with Tukey's correction).

c. Percent dauers amongst *ilc-17.1* (syb5296) X deletion mutants and wildtype (N2) larvae on 20mM Skim Milk powder and 0.26mM L-Glutamine at 25°C. *n*= 3 experiments. ns, not significant, (unpaired t-test).

d. Percent dauers amongst *ilc-17.1* (syb5296) X deletion mutants and wildtype (N2) larvae on 50mM glucose on Control (Ctrl; L4440) and *fgt-1* RNAi. *n*= 6 experiments. **p < 0.01, *p < 0.05. (unpaired t-test).

e. Average mRNA levels of GLUTs in *ilc-17.1* (syb5296) X deletion mutants relative to wildtype (N2). mRNA levels were determined relative to *pmp-3* and normalized to that in wildtype (N2). *n=3* experiments, 30 day-one adults each. *p < 0.05, (unpaired t-test).

Data in all graphs show mean ± s.e.m.

Figure S5

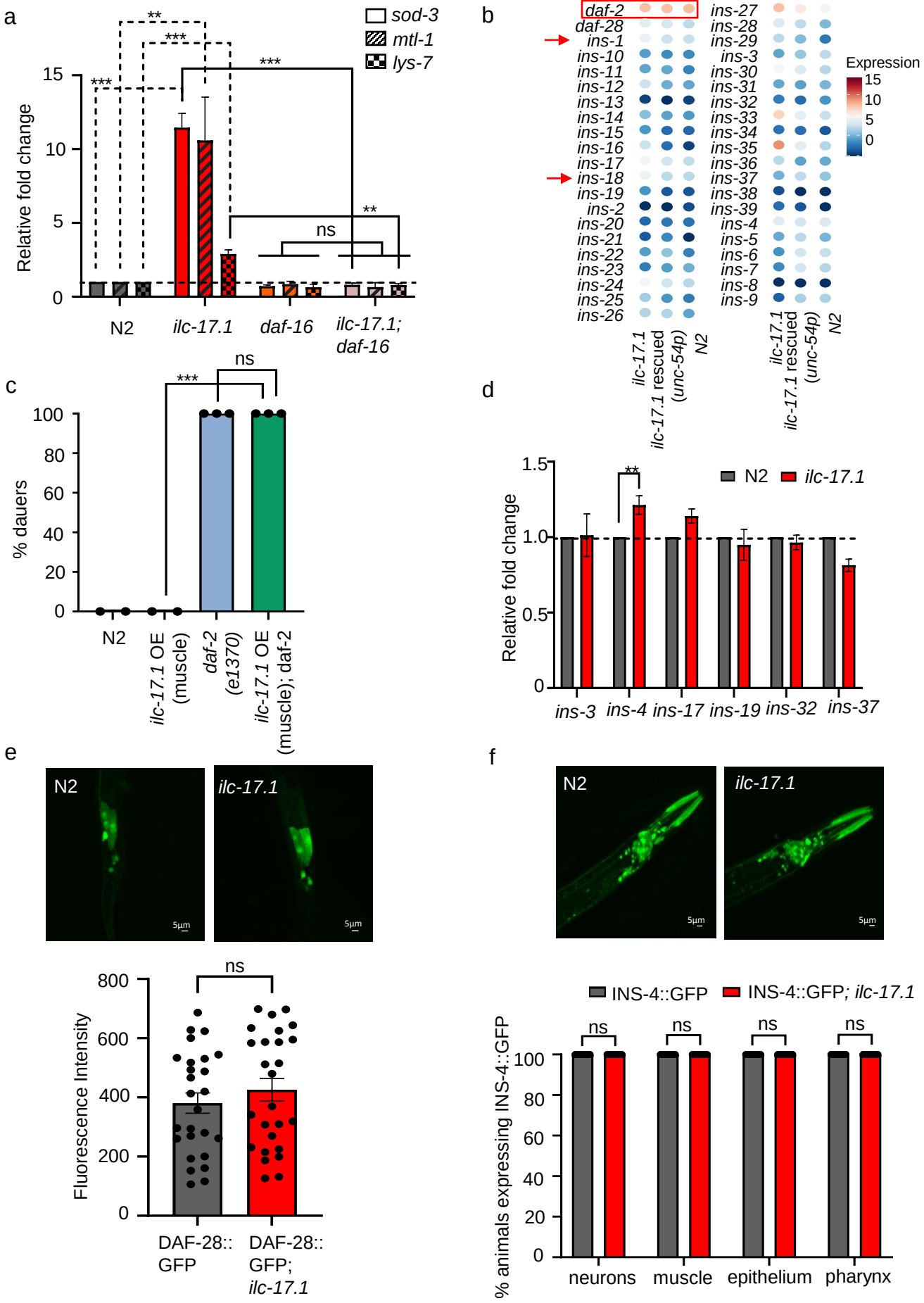
a
sod-3
mtl-1
lys-7
Relative fold change
N2
ilc-17.1
daf-16
ilc-17.1; daf-16
ns
b
Expression
daf-2
daf-28
ins-1
ins-10
ins-11
ins-12
ins-13
ins-14
ins-15
ins-16
ins-17
ins-18
ins-19
ins-2
ins-20
ins-21
ins-22
ins-23
ins-24
ins-25
ins-26
ins-27
ins-28
ins-29
ins-3
ins-30
ins-31
ins-32
ins-33
ins-34
ins-35
ins-36
ins-37
ins-38
ins-39
ins-4
ins-5
ins-6
ins-7
ins-8
ins-9
ilc-17.1
ilc-17.1 rescued (unc-54p)
N2
c
% dauers
N2
ilc-17.1 OE (muscle)
daf-2 (e1370)
ilc-17.1 OE (muscle); daf-2
d
Relative fold change
N2
ilc-17.1
ins-3
ins-4
ins-17
ins-19
ins-32
ins-37
e
N2
ilc-17.1
5µm
Fluorescence Intensity
DAF-28::GFP
DAF-28::GFP; ilc-17.1
f
INS-4::GFP
INS-4::GFP; ilc-17.1
% animals expressing INS-4::GFP
neurons
muscle
epithelium
pharynx

Supplementary Figure S5: ILC-17.1 deficiency does not act through reduced insulin signaling (rIS) to induce dauer arrest.

a. Average *sod-3, mtl-1, and lys-7* mRNA levels in 40 hr. old larvae grown at 20°C. mRNA levels were determined relative to *pmp-3* and normalized to that in wildtype (N2). *n*=3 experiments. ***p < 0.001, **p < 0.01, (unpaired t-test).

b. Heatmap depicting expression levels (log_2 normalized counts) of *daf-2* (boxed) and insulin ligands in the *ilc-17.1 (syb5296)* X deletion mutants, *ilc-17.1 (syb5296)* X deletion mutants rescued by ILC-17.1::FLAG in the body wall muscle, and wildtype (N2). Arrows highlight lack of changes in *ins-1* and *ins-18* mRNA. RNA-seq data from larvae grown for 34-36 hrs. at 25°C.

c. Percent dauers; overexpression of ILC-17.1::FLAG in the body wall muscle of *daf-2*(e1370)III strains does not rescue their dauer arrest. *n*=3 experiments. ***p < 0.001, ns, not significant (unpaired t-test).

d. Average mRNA levels (insulins) in 34-36 hr. larvae grown at 25°C. mRNA levels were determined relative to *pmp-3* and normalized to that in wildtype (N2). *n*=3 experiments. **p < 0.001, (unpaired t-test).

e. **Top**: Representative micrographs showing DAF-28::GFP expression in the last intestinal cell of 34-36hr larvae at 25°C of *ilc-17.1 (syb5296)* X deletion mutants and wildtype (N2). Images are projections of confocal z-planes. Scale bar: 5µm. **Bottom:** Quantification of fluorescent intensity of DAF-28: GFP. *n*=3 experiments. The fluorescent intensity of DAF-28::GFP in individual animals is depicted. ns, not significant (unpaired t-test).

775 **f.** **Top**: Representative micrographs showing INS-4: GFP expression in the pharyngeal
776 muscle, neurons, and pharynx of 34-36hr larvae at 25°C in *ilc-17.1 (syb5296)* X deletion
777 mutants and wildtype (N2). Images are projections of confocal z-planes. Scale bar: 5µm.
778 **Bottom:** Percent larvae that expressed GFP in the different tissues where INS-4 is known
779 to be expressed. *n*=3 experiments of 5-10 larvae of each strain. ns, not significant
780 (unpaired t-test).

781

782 Data in all graphs show mean ± s.e.m.

Figure S6

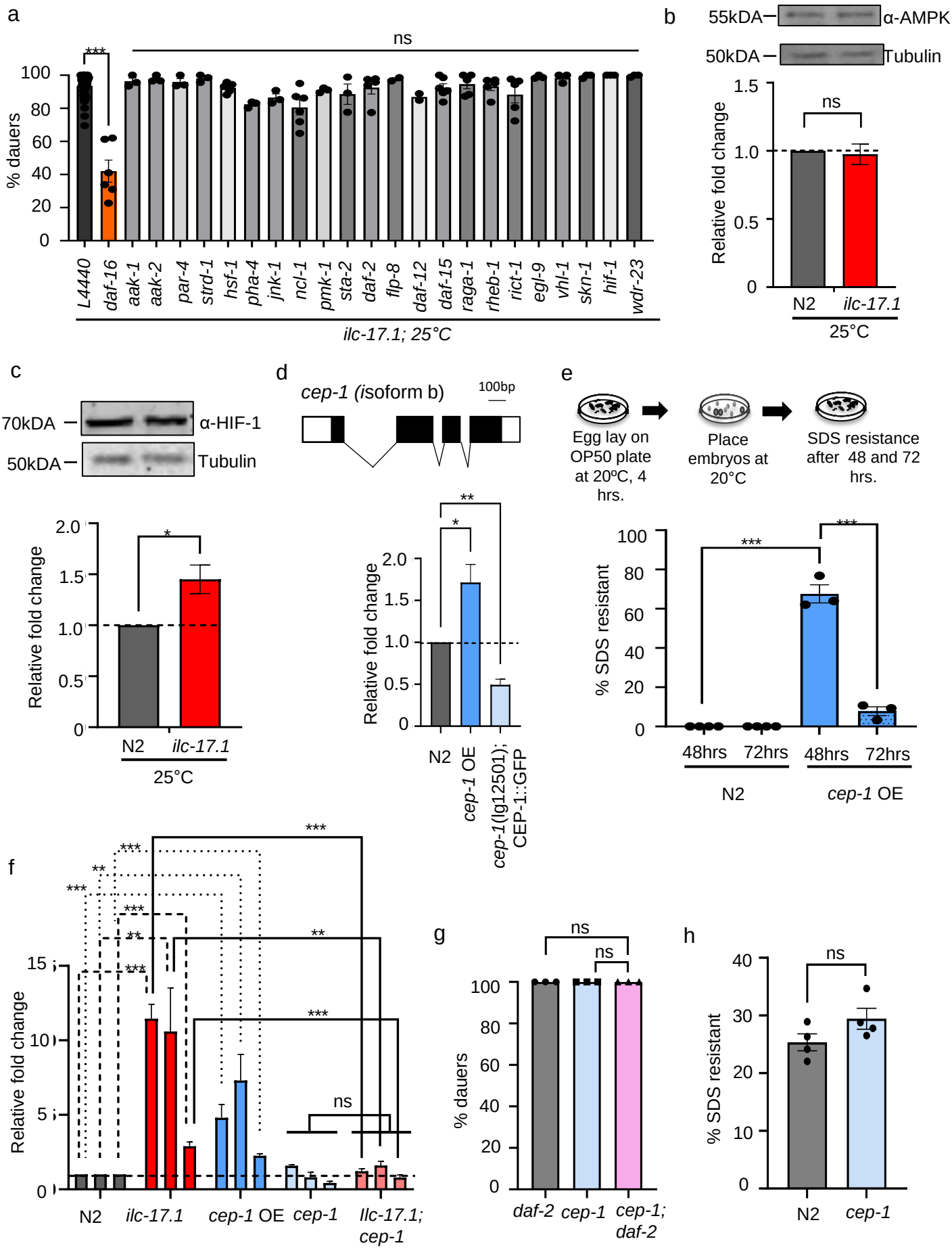
a
ns
***
100
80
60
40
20
0
% dauers
L4440
daf-16
aak-1
aak-2
par-4
strd-1
hsf-1
pha-4
jnk-1
ncl-1
pmk-1
sta-2
daf-2
flp-8
daf-12
daf-15
raga-1
rheb-1
rict-1
egl-9
vhl-1
skn-1
hif-1
wdr-23
ilc-17.1; 25°C
b
55kDA
α-AMPK
50kDA
Tubulin
1.5
1.0
0.5
0
Relative fold change
ns
N2
ilc-17.1
25°C
c
70kDA
α-HIF-1
50kDA
Tubulin
2.0
1.5
1.0
0.5
0
Relative fold change
*
N2
ilc-17.1
25°C
d
cep-1 (isoform b)
100bp
**
*
2.0
1.5
1.0
0.5
0
Relative fold change
N2
cep-1 OE
cep-1(lg12501); CEP-1::GFP
e
Egg lay on OP50 plate at 20ºC, 4 hrs.
Place embryos at 20°C
SDS resistance after 48 and 72 hrs.
***
***
100
80
60
40
20
0
% SDS resistant
48hrs
72hrs
48hrs
72hrs
N2
cep-1 OE
f
***
***
**
***
**
***
**
***
***
15
10
5
0
Relative fold change
ns
N2
ilc-17.1
cep-1 OE
cep-1
Ilc-17.1; cep-1
g
ns
ns
100
80
60
40
20
0
% dauers
daf-2
cep-1
cep-1; daf-2
h
ns
40
30
20
10
0
% SDS resistant
N2
cep-1

Supplementary Figure S6: ILC-17.1 deficiency triggers CEP-1/p53 activation to induce dauer arrest.

a. Percent dauers in *ilc-17.1* (syb5296) X deletion mutant larvae following RNAi-mediated downregulation of several genes known to interact with DAF-16. *daf-16* RNAi was used as positive control. *n=3*-5 experiments. ***p < 0.001, ns, not significant (unpaired t-test).

b. **Top:** Representative Western blot showing (upper panel) phospho-AMPK levels in *ilc-17.1* (syb5296) X deletion mutant larvae and wildtype (N2); (lower panel) tubulin, loading control. **Bottom:** Quantification of Phospho-AMPK levels relative to tubulin and normalized to control animals. *n*=3 experiments. ns, not significant (unpaired t-test).

c. **Top:** Representative Western blot showing (upper panel) HIF-1 in *ilc-17.1 (syb5296)* X deletion mutant larvae and wildtype (N2); (lower panel) tubulin, loading control. **Bottom:** Quantification of HIF-1 levels relative to tubulin and normalized to control animals. *n*=3 experiments. *p < 0.05 (unpaired t-test).

d. **Top:** Schematic of *cep-1* mRNA, isoform b. **Bottom:** Average *cep-1* isoform b mRNA levels in 34-36 hr. larvae grown at 25°C. mRNA levels were determined relative to *pmp-3* and normalized to that in wildtype (N2). *n*=3 experiments, 400 larvae each. **p < 0.001, *p < 0.05 (unpaired t-test).

e. **Top:** Schematic of SDS treatment to assess dauer formation at 20°C. Percent of wildtype (N2) and *cep-1* overexpressing larvae (*cep-1* OE) that enter a dauer state during development, 48 hours and 72 hrs. post-hatching at 20°C. *n*=3 experiments. ***p < 0.001, (analysis of variance (ANOVA) with Tukey's correction).

f. Average *sod-3, mtl-1, and lys-7* mRNA levels in 40 hr. larvae grown at 20°C. mRNA levels were determined relative to *pmp-3* and normalized to that in wildtype (N2). *n*=6-10 experiments. ***p < 0.001, **p < 0.01, ns, not significant. (unpaired t-test).

g. Percent dauers in *daf-2* (e1370) and *daf-2* (e1370); *cep-1* (gk138). Note: no rescue. *n*=3 experiments. ns, not significant. (unpaired t-test).

h. Percent high temperature (27.5 °C; HID phenotype) dauers in wildtype (N2) and *cep-1* deletion mutants *cep-1(gk138)*. *n*=4 experiments. ns, not significant. (unpaired t-test).

Data in all graphs show mean ± s.e.m.

Figure S7

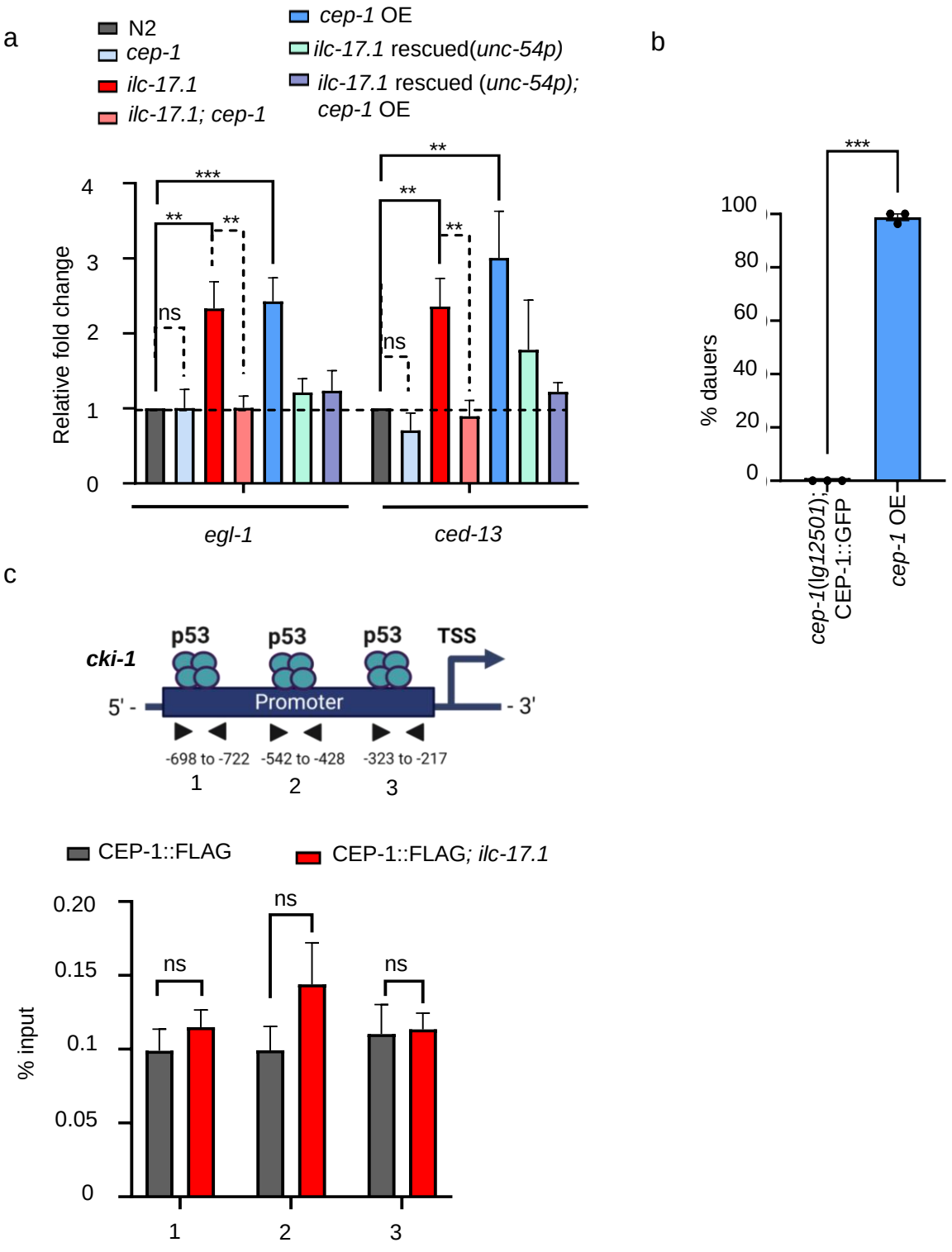
a
N2
cep-1
ilc-17.1
ilc-17.1; cep-1
cep-1 OE
ilc-17.1 rescued(unc-54p)
ilc-17.1 rescued (unc-54p); cep-1 OE
Relative fold change
egl-1
ced-13
b
% dauers
cep-1(lg12501); CEP-1::GFP
cep-1 OE
c
cki-1
p53
TSS
Promoter
5' -
- 3'
-698 to -722
-542 to -428
-323 to -217
CEP-1::FLAG
CEP-1::FLAG; ilc-17.1
% input
ns

Supplementary Figure S7: CEP-1/p53 is active even under optimal growth conditions in *ilc-17.1* deletion mutants and indirectly upregulates the p21 ortholog, *cki*-1.

a. Average *egl-1* and *ced-13* mRNA levels in 40 hr. larvae grown at 20°C. mRNA levels were determined relative to *pmp-3* and normalized to that in wildtype (N2). *n*=6-7 experiments. ***p < 0.001, **p < 0.01, ns, not significant (unpaired t-test).

b. Percent dauers upon expression of a functional, rescuing CEP-1::GFP translational fusion in a wildtype (N2) background with intact endogenous *cep-1* gene [i.e. *cep-1* overexpression; *cep-1* OE], versus expression of the same construct in a *cep-1* deletion background, *cep-1*(lg12501), where endogenous CEP-1 is not expressed [*cep-1*(lg12501); CEP-1::GFP]. mRNA levels in **Supplementary Figure S6d**. *n*=3 experiments. ***p < 0.001. (unpaired t-test).

c. CEP-1 occupancy (expressed as percent input) in 34-36 hr. larvae grown at 25°C, measured at three promoter proximal regions of *cki-1* (Schematic on top). Strains used: CEP-1::FLAG expressing animals in control wild-type background (Ctrl), in *ilc-17.1*(syb5296) X background. *n*=4 experiments. ns, not significant. (unpaired t-test).

Data in all graphs show mean ± s.e.m.

Figure S8

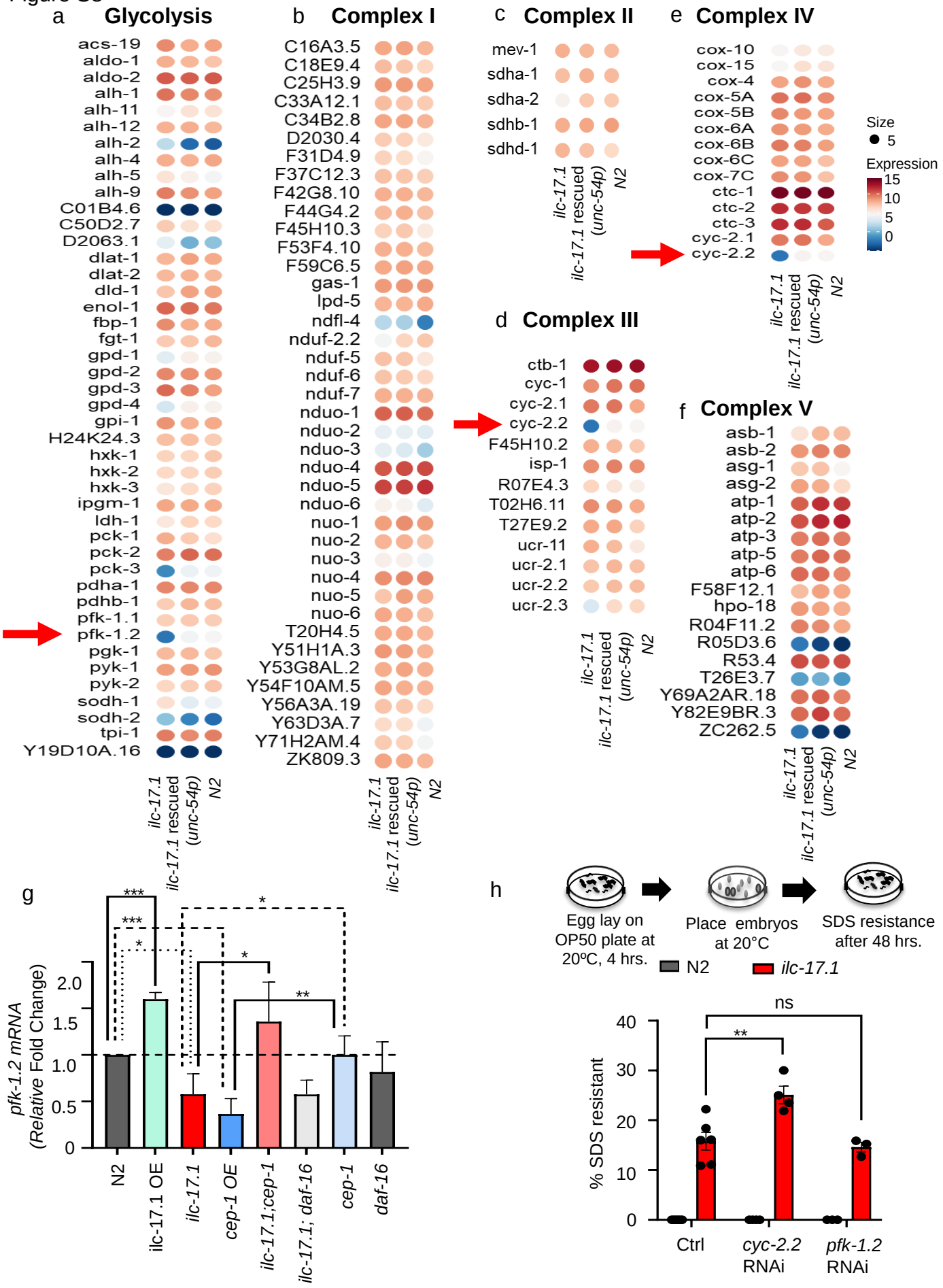
a Glycolysis
acs-19
aldo-1
aldo-2
alh-1
alh-11
alh-12
alh-2
alh-4
alh-5
alh-9
C01B4.6
C50D2.7
D2063.1
dlat-1
dlat-2
dld-1
enol-1
fbp-1
fgt-1
gpd-1
gpd-2
gpd-3
gpd-4
gpi-1
H24K24.3
hxk-1
hxk-2
hxk-3
ipgm-1
ldh-1
pck-1
pck-2
pck-3
pdha-1
pdhb-1
pfk-1.1
pfk-1.2
pgk-1
pyk-1
pyk-2
sodh-1
sodh-2
tpi-1
Y19D10A.16
ilc-17.1
ilc-17.1 rescued (unc-54p)
N2
b Complex I
C16A3.5
C18E9.4
C25H3.9
C33A12.1
C34B2.8
D2030.4
F31D4.9
F37C12.3
F42G8.10
F44G4.2
F45H10.3
F53F4.10
F59C6.5
gas-1
lpd-5
ndfl-4
nduf-2.2
nduf-5
nduf-6
nduf-7
nduo-1
nduo-2
nduo-3
nduo-4
nduo-5
nduo-6
nuo-1
nuo-2
nuo-3
nuo-4
nuo-5
nuo-6
T20H4.5
Y51H1A.3
Y53G8AL.2
Y54F10AM.5
Y56A3A.19
Y63D3A.7
Y71H2AM.4
ZK809.3
c Complex II
mev-1
sdha-1
sdha-2
sdhb-1
sdhd-1
d Complex III
ctb-1
cyc-1
cyc-2.1
cyc-2.2
F45H10.2
isp-1
R07E4.3
T02H6.11
T27E9.2
ucr-11
ucr-2.1
ucr-2.2
ucr-2.3
e Complex IV
cox-10
cox-15
cox-4
cox-5A
cox-5B
cox-6A
cox-6B
cox-6C
cox-7C
ctc-1
ctc-2
ctc-3
cyc-2.1
cyc-2.2
Size
5
Expression
15
10
5
0
f Complex V
asb-1
asb-2
asg-1
asg-2
atp-1
atp-2
atp-3
atp-5
atp-6
F58F12.1
hpo-18
R04F11.2
R05D3.6
R53.4
T26E3.7
Y69A2AR.18
Y82E9BR.3
ZC262.5
g
pfk-1.2 mRNA (Relative Fold Change)
2.0
1.5
1.0
0.5
0
***
***
*
*
*
**
N2
ilc-17.1 OE
ilc-17.1
cep-1 OE
ilc-17.1;cep-1
ilc-17.1; daf-16
cep-1
daf-16
h
Egg lay on OP50 plate at 20ºC, 4 hrs.
Place embryos at 20°C
SDS resistance after 48 hrs.
N2
ilc-17.1
% SDS resistant
40
30
20
10
0
ns
**
Ctrl
cyc-2.2 RNAi
pfk-1.2 RNAi

Supplementary Figure S8: ILC-17.1 deficiency and CEP-1/p53 activation modulates key glucose metabolic enzymes.

a-f. Heatmap depicting expression levels (log_2 normalized counts) of glycolysis and mitochondrial OXPHOS genes in the *ilc-17.1* (syb5296) X deletion mutants, *ilc-17.*1 (syb5296) X deletion mutants rescued by the overexpression of ILC-17.1::FLAG in the body wall muscle, and wildtype (N2). Arrows highlight decreases in *pfk-1.2* and *cyc-2.2* mRNA levels in *ilc-17.1* mutants. RNA-seq data was collected as previously described.

g. Average *pfk-1.2* mRNA levels in 34-36 hr. old larvae grown at 25°C. mRNA levels were determined relative to *pmp-3* and normalized to that in wildtype (N2). *n*=4-6 experiments. ***p < 0.001, **p < 0.01, *p < 0.05. (unpaired t-test).

h. **Top:** Schematic of SDS treatment to assess dauer formation at 20°C. Percent of wildtype (N2) and *ilc-17.1* (syb5296) X deletion mutants larvae that enter a dauer state at 20°C when subjected to control (L4440; Ctrl), *cyc-2.2* and *pfk-1.2* RNAi. SDS-resistant dauers scored 48 hours post-hatching. n=3-4 experiments. **p < 0.01, (analysis of variance (ANOVA) with Tukey's correction).

Data in all graphs show mean ± s.e.m.

Figure S9

a

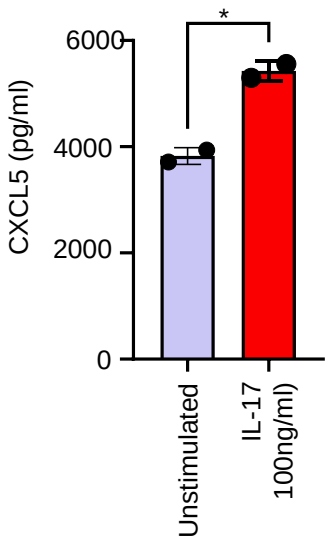

Supplementary Figure S9: rIL-17 induces the expected cytokine response in human epithelial cells.

a. Soluble CXCL5 levels in the supernatant of A459 epithelial cells stimulated for 18hrs with rIL-17 measured by ELISA. Data is a summary of 2 independent experiments, performed in triplicates. *p<0.05, (unpaired t-test). Data show mean ± s.e.m.

Materials and Methods

C. elegans strains

C. elegans strains used in this study are listed in Table 1. Strains were procured from Caenorhabditis Genetics Center (CGC, Twin Cities, MN), generated in the laboratory or generated by Suny Biotech (Suzhou, Jiangsu, China 215028).

Table 1

Strain Name	**Gene name**	**Source**	**Additional information**
N2, *C. elegans* var *Bristol*	N2, Wild-type	Caenorhabditis Genetics Center	
TJ1	*cep-1* (gk138) I	Caenorhabditis Genetics Center	
CF1038	*daf-16* (mu86) I	Caenorhabditis Genetics Center	
TG12	*cep-1*(lg12501) I*; unc-119* (ed4) III; gtIs1 [CEP-1::GFP + *unc-119* (+)]	Caenorhabditis Genetics Center	Pcep-1::CEP-1(let-585 3'UTR)::GFP; from construct pRH53
CB1370	*daf-2* (e1370) III	Caenorhabditis Genetics Center	
VEP024	praEx021 (*ilc-17.1*p::*ilc-17.1* cDNA::3XFLAG::*ilc-17.1* 3'UTR; p*myo-2*::mCherry::*unc-54* 3'UTR)	Prahlad Lab	ILC-17.1 overexpression under its own promoter and 3'UTR

VEP031	praEx022 (*unc-54*p::*ilc-17.1* cDNA::3XFLAG::*tbb-2* 3'UTR; p*dat-1*::GFP::*unc-54* 3'UTR)	Prahlad Lab	ILC-17.1 overexpression under the muscle promoter and 3'UTR
VEP032	*ilc-17.1* (syb5296) X	Prahlad Lab/ SunyBiotech	*ilc-17.1* deletion, 2173bp deletion, and the 15bp and 127bp sequences were left in the 5' and 3' deletion end, respectively of the 2135 bp *ilc-17.1* gene
VEP033	*ilc-17.1* (syb5296) X; praEx022 (*unc-54*p::*ilc-17.1* cDNA::3XFLAG ::*tbb-2* 3'UTR; p*dat-1*::GFP::*unc-54* 3'UTR)	Prahlad Lab	ILC-17.1 paracrine rescue of *ilc-17.1* deletion
VEP034	*ilc-17.1* (syb5296)X; *cep-1* (gk138) I	Prahlad Lab	
VEP035	*ilc-17.1* (syb5296); *daf-16* (mu86) I	Prahlad Lab	
VEP036	*unc-119* (ed4); gtIs1 [CEP-1::GFP + *unc-119* (+)]	Prahlad Lab	CEP-1 overexpression (ref: [65])
VEP037	*ilc-17.1* (syb5296); praEx022 (*unc-54*p::*ilc-17.1* cDNA:: 3XFLAG::*tbb-2* 3'UTR; p*dat-1*::GFP::*unc-54*	Prahlad Lab	IL-17.1 overexpression; CEP-1/p53 overexpression

	3'UTR); *unc-119* (ed4); gtIs1 [CEP-1::GFP + *unc-119* (+)]		
VEP038	*ilc-17.1* (syb5296); praEx022 (*unc-54*p::*ilc-17.1* cDNA:: 3XFLAG::*tbb-2* 3'UTR; p*dat-1*::GFP::*unc-54* 3'UTR); *daf-2* (e1370) III	Prahlad Lab	
VEP039	*daf-2* (e1370) III; *cep-1* (gk138) I	Prahlad Lab	
VEP040	*cep-1* ((syb6099) [*cep-1*::3XFLAG]) I	Prahlad Lab/ SunyBiotech	Endogenous *cep-1* 3X FLAG tagged at C-terminus
VEP041	*ilc-17.1* (syb5296)X ; *cep-1* (pra02 [*cep-1*::3XFLAG]) I	Prahlad Lab	
VEP042	praEx022 (*unc-54*p::*ilc-17.1* cDNA::3XFLAG::*tbb-2* 3'UTR; p*dat-1*::GFP::*unc-54* 3'UTR); *ilc-17.1* (syb5296) X ; *cep-1* (pra02 [cep-1::3XFLAG]) I	Prahlad Lab	
VEP043	*ilc-17.1* (pra03 [*ilc-17.1*::SL2::mCherry]) X	Prahlad Lab/ SunyBiotech	
VEP044	*ilc-17.1* (pra04 [*ilc-17.1*::3xHA]) X	Prahlad Lab/ SunyBiotech	
VEP045	*ilcr-2* (pra05 [*ilcr-2*::SL2::GFP]) II	Prahlad Lab/ SunyBiotech	

Generation of CRISPR strains

CRISPR/Cas9 was used to create following *C. elegans* strains:

Background Strain	**Type of editing**	**Description/position of editing**	**Gene**	**Resulting strain**
N2, *C. elegans* var Bristol	Deletion (syb5296)	2173bp deletion, and the 15bp and 127bp sequences were left in the 5' and 3' deletion end, respectively of the 2135 bp *ilc-17.1* gene	(*ilc-17.1*)X	VEP032
N2, *C. elegans* var Bristol	Insertion; *SL2::mCherry*	C'-terminus	(*ilc-17.1*)X	VEP043
N2, *C. elegans* var Bristol	Insertion; 3X HA	C'-terminus	(*ilc-17.1*)X	VEP044
N2, *C. elegans* var Bristol	Insertion; SL2::GFP	C'-terminus	(*ilcr-2*)II	VEP045
N2, *C. elegans* var Bristol	Insertion; 3X FLAG	C'-terminus	(*cep-1*)I	VEP040

Generation of transgenic strains

i) Generation of *cep-1* overexpression strain

TG12 (*cep-1*(lg12501) I; *unc-119* (ed4) III; [CEP-1::GFP + *unc-119* (+)]) is a strain that expresses functional CEP-1 tagged with GFP, as determined by the rescue of *cep-1*(lg1250) phenotype[68]. To overexpress CEP-1 we backcrossed the TG12 strain with wild-type (N2) worms and selected F2 progeny that were homozygous for the wild-type *cep-1* gene, lacked the *cep-1*(lg12501) I mutation (confirmed by PCR), and were homozygous for the CEP-1::GFP transgene (confirmed by 100% GFP expression amongst the F3 and F4 progeny). Overexpression of cep-1 mRNA was

verified by qPCR (Supplementary Figure S6d). The CEP-1::GFP construct was PCR amplified from the final transgenic VEP037 *C. elegans* strain, and sequence verified.

ii) Generation of ILC-17.1 overexpression strain under its own promoter and 3'UTR

To generate the strain VEP024 – praEx021 [(*ilc-17.1*p::*ilc-17.1* (cDNA)::3xFLAG::*ilc-17.1* 3'UTR); p*myo-2*::mCherry::*unc-54* 3'UTR], which overexpressed *ilc-17.1* under the endogenous *ilc-17.1* promoter and *ilc-17.1* 3'UTR, we first amplified 3 kb of genomic sequence upstream of the translational start site (*ilc-17.1* promotor) and 1 kb of genomic sequence downstream from the translational stop codon (*ilc-17.1* 3' UTR). These regions were cloned using Gateway technology into pDONR221. *ilc-17.1* cDNA fused to C-terminal 3xFLAG sequence was synthesized as a gBlock (Integrated DNA technologies). These three fragments were then submitted for gene synthesis service through GenScript to generate the expression vector pUC57(*ilc-17.1*p:: *ilc-17.1* (cDNA)::3xFLAG:: *ilc-17.1* 3'UTR). All plasmids were sequence verified. The *ilc-17.1* expression vector was then injected at 97.5 ng/ul along with the co-injection marker pCFJ90 (p*myo-2*::mCherry::*unc-54* 3'UTR) at 2.5 ng/ul by InVivo Biosystems injection express service. Animals expressing mCherry were singled, lines transmitting the extrachromosomal array were established, and mCherry positive progeny were PCR verified to ensure they were transmitting *ilc-17.1*p:: *ilc-17.1* (cDNA)::3xFLAG:: *ilc-17.1* 3'UTR. These lines were then harvested for Western blot to verify expression of protein.

iii) Generation of ILC-17.1 overexpression strain under the *unc-54* muscle promoter and *tbb-2* 3'UTR

To generate VEP031, we overexpressed ILC-17.1 under muscle promoter by fusing - [(*unc-54*p:: *ilc-17.1* (cDNA)::3xFLAG] which was synthesized as a gBlock (Integrated DNA technologies) and *tbb-2* 3' UTR which was amplified from genomic DNA. The two fragments were cloned into pUC19 plasmid as the backbone using Gibson assembly[103] to create the overexpression plasmid [(*unc-54*p:: *ilc-17.1* (cDNA)::3xFLAG::*tbb-2* 3'UTR); p*dat-1*::ssmito] and sequence verified. The construct was injected at 100 ng/ul along with the co-injection marker

that expressed GFP in the dopaminergic neurons under a *dat-1* promoter [p*dat-1*], at 10 ng/ul into wildtype (N2) worms. Animals expressing GFP in their dopaminergic neurons were singled, lines were established, and GFP-positive progeny were PCR verified to ensure that they were also transmitting harbored the *ilc-17.1* transgene. These lines were then harvested for Western blot to verify expression of protein.

Growth conditions for *C. elegans* strains

All strains were grown and maintained at 20°C unless otherwise mentioned. Animals were grown in 20°C incubators (humidity controlled) on 60mm nematode growth media (NGM) plates by passaging 8-15 L4s (depending on the strain) onto a fresh plates. Extra care was taken to ensure equal worm densities across all strains. Animals were fed *Escherichia coli* OP50 obtained from Caenorhabditis Genetics Center (CGC) that were seeded (OD_{600}=1.5 and this was strictly maintained throughout the experiments) onto culture plates 2 days before use. The NGM plate thickness was controlled by pouring 8.9ml of autoclaved liquid NGM per 60mm plate. Laboratory temperature was maintained at 20°C and monitored throughout. For all experiments, age-matched day-one hermaphrodites, or larvae timed to reach specific developmental stages as mentioned in the figure legend, were used.

For all experiments with larvae, the timings were adjusted to account for the differences in growth rates at different temperatures. Thus, at 25°C, larvae were harvested 30-36 hrs. post bleach hatch or egg lay, and at 20°C, larvae were harvested 40 hrs. post bleach hatch or egg lay.

Obtaining synchronized embryos by 'bleach-hatching'

Bleach-hatching' was performed as previously described[94]. Populations of 250-300 gravid adults were generated by passaging L4s, as described above. These plates were used for obtaining synchronized embryos by bleach-induced solubilization of the adults. Specifically, animals were

washed off the plates with 1X PBS and pelleted by centrifuging at 2665Xg for 30s. The PBS was removed carefully, and worms were gently vortexed in the presence of bleaching solution [250µl 1N NaOH, 200µl standard (regular) bleach and 550µl sterile water] until all the worm bodies had dissolved (approximately 5-6 minutes), and only eggs were viable. The eggs were pelleted by centrifugation (2665Xg for 45s), bleaching solution was carefully removed and then embryos were washed with sterile water 3-4 times and counted under the microscope. The desired number of embryos were seeded on fresh OP50 plates and allowed to grow at 20°C or 25°C for specific time periods depending on the experimental need. If >5% eggs remained unhatched, these plates were discarded.

Dauer Assay

Embryos were allowed to hatch and grow on OP50 plates at 20°C or 25°C for this assay. Embryos were generated according to one of the following two methods: (i) Day-one gravid adults that had grown under normal culture conditions (on OP50 at 20°C) were bleach dissolved as described above, and ~50-100 embryos obtained from these gravid adults were seeded on fresh OP50 plates or (ii) day-one gravid adults were allowed to lay eggs on fresh OP50 (or RNAi) plates for 2-4 hours at 20°C, the adults were removed. and then embryos were allowed to develop at 20°C or 25°C under humified condition for 48-72 hrs. The number of larvae that arrested as dauers (determined by phenotype and/or resistance to 1%SDS) and those that developed into L4s or adults were counted and percentage of dauers was calculated. The total number of embryos in each plate was ~50-100. Each experiment was performed in triplicate or more.

SDS treatment

Larvae were washed off the dauer assay plates, washed 1X with PBS to remove bacteria, treated with 1% sodium dodecyl sulfate (SDS) for 30 minutes, washed again with M9, and then transferred

onto a fresh plate. Larvae could be scored easily as dead/dissolved or as live dauer larvae (based on their phenotype, and movement).

RNAi mediated downregulation of genes

All RNAi clones used were verified by sequencing, and plates were seeded with RNAi bacteria for a maximum of two days before being used. Day-one gravid adults grown on OP50 were allowed to lay eggs on RNAi-bacteria seeded plates for 2-4 hours at 20°C. The adults were then removed, and the embryos were transferred to 25°C (or kept at 20°C) under humified condition for 48-72 hrs. The number of larvae that arrested as dauers (determined by phenotype and/or resistance to 1%SDS) and those that developed into L4s or adults were counted and percentage of dauers was calculated.

Exposure to food [OP50] availability

Gravid day-one *ilc-17.1*(pra03 [*ilc-17.1*::SL2::mCherry]) X adults or *ilc-17.1*(pra04 [*ilc-17.1*::3xHA]) X adults were bleach dissolved and embryos were placed either on empty plates with no food or NGM plates seeded with OP50 and allowed to grow for 24-36 hours at 25°C. To observe mRNA expression of *ilc-17.1, ilc-17.1*(pra03 [*ilc-17. 1:*SL2::mCherry]) X larvae were anesthetized with 1mM levamisole, mounted on 1% agarose pads, and imaged using a Confocal SPE microscope using optimal settings. mCherry expression served to mark cells that expressed *ilc-17.1* mRNA. To identify where ILC-17.1 protein was expressed prior to food exposure, and after food exposure, 24-36 hour *ilc-17.1*(pra04 [*ilc-17.1*::3xHA]) X larvae were fixed and immunostained using Bouin's Tube Fixation method (see below).

Immunofluorescence

Nematodes were fixed and immunostained using a modification of the Bouin's Tube Fixation method [104]. Worms were fixed for 30 min. at room temperature (RT) in 400 µl Bouin's fix (Sigma

Aldrich) + 600 µl methanol and 10 µl β-mercaptoethanol by tumbling, freeze cracked three times in liquid nitrogen and again tumbled for 30 mins at RT. For permeabilization, the fixative was removed and exchanged for borate-Triton-βmercaptoethanol (BTB: 1xBorate Buffer, 0.5% Triton and 2% β-mercaptoethanol) solution. Worms were tumbled 3 times for 1 hour each in fresh BTB solution at RT. Worms were washed with PBS-0.05% Tween and incubated in block-solution (5% BSA). Staining with primary antibody was performed overnight at 4 °C, incubation with secondary antibody (Donkey anti-Mouse Alexa Fluor 488, 1:2000) for 2-4 hours at RT. All antibody dilutions were performed using antibody buffer containing 5% BSA. Samples were mounted onto glass slides using VECTASHIELD antifade mounting medium (Vector Laboratories, Burlingame, CA, USA).

Primary antibodies used: (i) Monoclonal ANTI-FLAG M2, Sigma Aldrich, 1:500, (ii) Mouse anti-HA antibody, Thermofisher; 2-2.2.14, at 1:1000), (iii) anti β-Actin, Cell Signaling Technology, #4967, 1:1000.

Chemotaxis

Chemotaxis assay was performed on 9 cm petri dishes containing NGM. Two marks were made on the back of the plate at opposite sides of the plate about 0.5 cm from the edge of the agar. About 5 µl of attractant diluted in water was placed on the agar over one mark, and 5 µl of water was placed as the control over the opposite mark. Attractants and concentrations used are listed in drugs and metabolites section. 5 ul sodium azide with the concentration of 1M was also placed at both the attractant source and the control source. This drug could anesthetize animals within about a 0.5-cm radius of the attractant. Age synchronized day-one adult worms were transferred to the middle of the NGM plates at a point equidistant from the middle of each odorant. After 1 hr., the assay was quantified by counting the number of worms that had left the center origin a chemotaxis index was calculated [#Odor - #Control] / [#Odor + #Control]. Each repeat consisted of 50 worms, and experiments were repeated a minimum of three times.

Measuring Pharyngeal pumping

Synchronized day-one adults were singled onto NGM plates seeded with OP50, and onto plates without OP50. Pharyngeal pumping rates were determined by recording the pharyngeal region of animals by video using a Leica S9i digital stereo microscope at 5X magnification and slowing down the video to manually count the number of 'pumps' in 10 seconds, three times per animal. The mean of these pumps was determined and the number of pumps/minute calculated. One complete cycle of synchronous contraction and relaxation of the corpus and the terminal bulb was counted as a pump.

Feeding of fluorescent latex beads

Overnight 5ml OP50 culture LB was pelleted and resuspended in fresh 0.5ml LB to concentrate bacteria. 1 µl of fluorescent beads of 0.5µm mean particle size that mimic size of *E. coli*. (Sigma L3280, red fluorescence) was added to 1 ml of concentrated OP50 [1:1000 ratio (v/v)], and 100ul of the mixture was seeded onto NGM plates [105]. Synchronized day-one adults were allowed to lay eggs on the bead containing plates for 2 hours at 20°C and then removed. After 40 hours, larvae were picked onto 1% agarose pads on glass slides and anesthetized using 10mM levamisole. Z-stack images of the larvae were taken on Leica TCS SPE confocal microscope and number of beads within a set area near the tail region per larvae was quantified.

Fluorescence Image analysis

ImageJ (Fiji) v1.53i was used for measuring fluorescence intensity as follows: single planes [, DAF-16::GFP, CEP-1::GFP, TG12] or projections of z-planes [DAF-28, INS-4, fluorescent latex beads] were used for measuring fluorescence intensity. The region of interest was circled using the circle selection tool. The mean fluorescence intensity of each circled area was recorded using

the measurement tool. When appropriate, the background fluorescence intensity was measured and subtracted. Quantification of measurements was done in Microsoft excel/GraphPad.

Drug and metabolite treatment

The following drugs or metabolites were used:

Drug/metabolite	Source	Final concentration
Glucose	Research products International	50/100mM
2-Deoxy-d-glucose	R&D systems	50mM
Mitotempo	Millipore sigma	0.1mM
L-Glutamine	Sigma-Aldrich	0.26mM
Skim Milk powder	HyVee - instant nonfat dry milk	20mM
Diacetyl	Sigma-Aldrich	0.01% v/v
Lysine	Sigma-Aldrich	1M

The drug solution (0.5 ml) was spread onto NGM agar plates containing an OP50 lawn and left for 1 hr. to dry or used for chemotaxis assays as described. Age synchronized day-one adult worms were transferred to the middle of the NGM plates for 4 hrs. and dauer assay were performed as described. Sterile water was used as control

RNA-sequencing and Data analysis

a) RNA isolation, library preparation and sequencing

Day-one adult worms were bleach-hatched and ~3200 eggs/genotype (~800 eggs/plate and 4 plates/genotype) were seeded on fresh OP50 plates and allowed to grow for 30-34 hrs. at 25°C. Worms were washed with sterile water and total RNA was extracted from

biological triplicates using the Direct-zol RNA Miniprep Kits (catalog no. R2050, Zymo Research). Libraries were prepared using the Illumina Stranded Total RNA Prep with Ribo-Zero Plus, for rRNA depletion (catalog no. 20040525, Illumina). Samples were sequenced in one lane of the Illumina NovaSeq 6000, generating 2x150bp paired-end reads.

b) RNA-seq analysis

The quality of the RNA sequences was assessed with FastQC. Adapters and sequence reads with a quality lower than Q25 were trimmed by using Trimgalore [106](v0.67). Ribosomal RNA (rRNA) contamination was filtered with sortmeRNA[107] (version 4.3.4). Sequencing reads were aligned to the *C. elegans* genome (WBcel235[108]) using the Star aligner[109] (v2.7.9a) and then the aligned reads were quantified with FeatureCounts v2.0.1 from the R package Rsubread[110] . Differential expression analysis was performed using DESeq2[111] and genes with FDR corrected p-value of < 0.05 were considered significant. Pairwise distance analysis (sample-to-sample) was performed by using normalized counts coupled with the variance stabilization transformation (VST) on the complete set of genes and calculating the Euclidean distance between the replicates. The microarray data for the *C. elegans* dauer stage was obtained from the Supplementary Table 1 of the study by Wang, J. & Kim (2003)[32]. The expression values of the dauer stage were defined as the dauers expression (fold-change) at 0hr relative to the mixed staged reference RNA. Sequences IDs from the array were converted to standard gene nomenclature using Simplemine in Wormbase[112]. The correlation between the expression at the dauer stage and the fold change in expression in the *ilc-17.1* deletion mutant relative to the wild type, was determined by performing a Spearman

Rank Test. The correlation test was performed in all genes present in both datasets and in a subset of the genes identified as collagens.

c) Functional analysis

Gene ontology analysis (GO) and KEGG enrichment analysis was performed on the differentially expressed genes by using ClusterProfiler 4.0[113]. Terms with an FDR corrected p-value <0.05 were considered significant. The annotations were obtained from R package org.Ce.eg.db[114] (version 3.14) and the KEGG database[115]. The annotations of genes as part of the metabolic pathways were obtained from the database Wormpaths[91] and Heatmaps were done using the package Complexheatmap[116].

Progenitor blast cell (P cells) imaging and quantification.

Synchronized day-one adults were allowed to lay eggs on OP50 plates for 2 hours at 20°C and then removed. The plates were then placed at 25°C. After 15 hours, about 10 L1 larvae were picked onto 1% agarose pads on glass slides and anesthetized using 10mM levamisole. The brightest Z-plane showing P cells was imaged on Leica TCS SPE confocal microscope. Mean fluorescence of the first four visible P cells was averaged in each L1 larva.

DiO dye filling assay to identify amphid neurons

A stock dye solution containing 2mg/ml DiO (Molecular Probes, catalog # D-275) in dimethyl formamide is made and maintained under dark conditions. Day-one adult worms were transferred into an eppendorf tube with 1 ml of M9, spun down at 2000-3000 rpm and supernatant removed. Worms were resuspended in 1 ml of M9 and 5 microliter DiO stock sol (1:200 dilution) was added and incubated on a slow shaker for 2 hours at room temperature. Worms were spun down and washed with M9 twice before transferring them onto agar pads with 1mM levamisole to visualize by fluorescence using a Leica TCS SPE confocal microscope.

Dauer pharyngeal pumping

Synchronized day-one adults were allowed to lay eggs on OP50 plates for 2 hours at 20°C and then removed. The plates were then placed at 25°C, and larvae were allowed to arrest as dauers or grow into L4 larvae (RNAi treatment). On day 3, larvae that remained arrested as dauers were used to measure pharyngeal pumping rates using Zeiss Axio Observer.A1 at 40X magnification. Pumping rates were measured by counting the number of grinder movements in the terminal bulb per minute. The average of three biological replicates consisting of 10 dauer larvae each was quantified.

Scoring apoptotic nuclei with Acridine Orange

Acridine orange (AO) staining was performed as previously described (Hefel et al. 2021). AO staining to detect apoptotic germline cells was performed by picking 50 L4 animals to a fresh plate and allowing them to grow into day-one adults for 24 hours at 20°C prior to staining. For each trial, 10 mg/ml AO stain was freshly prepared and then diluted 1:400 with M9 buffer. Worms were then picked to a tube of the diluted AO stain, wrapped tightly with foil, and rotated at room temperature for 2 hours. After mixing, worms were transferred to a fresh OP50 plate and allowed to crawl away from residual AO stain before being picked to a droplet of 10 mM levamisole on a 1% agarose pad. A cover slip was added, and worms were imaged immediately using the Leica fluorescence microscope on 60x magnification. It was important to visualize AO within 10 mins after mounting animals on the pad. The number of AO stain positive cells found in 12 individual gonad arms per experiment were recorded for each sample.

Gamma irradiating *C. elegans* to activate CEP-1/p53

100 L4 larvae were picked onto an OP50 seeded plate, allowed to mature into day-one adults and exposed to 75 Gy gamma irradiation, and subsequently harvested for Western blot

analysis. To determine the number of AO positive apoptotic nuclei, at least 50 L4 larvae were exposed to 75 Gy gamma irradiation. The number of AO positive cells were scored 24 hrs. later, when animals had matured into day-one adults.

Western blot analysis

i. Western blot analysis of *C. elegans*

Western blot analysis was performed with 30–100 adult day-one animals, or approximately 400 30-36 hr. larvae as indicated. Animals were harvested in 15 µl of 1X PBS (pH 7.4), and 4X Laemmli sample buffer (catalog no. 1610737, Bio-Rad) supplemented with 10% β-mercaptoethanol was added and samples were boiled for 30 min. Whole-worm lysates were resolved on 12% SDS-PAGE gels and transferred onto nitrocellulose membrane (catalog no. 1620115, Bio-Rad). Membranes were blocked with Odyssey Blocking Buffer (part no. 927–50000, LI-COR). Immunoblots were imaged using LI-COR Odyssey Infrared Imaging System (LI-COR Biotechnology, Lincoln, NE). Mouse anti-FLAG M2 antibody (catalog no. F1804, RRID:AB_262044,_Sigma Aldrich) was used at 1:500 to detect CEP-1::FLAG. Mouse anti-HA antibody (Thermofisher; 2-2.2.14), was used at 1:1000 to detect ILC-17.1::HA. Rabbit monoclonal Phospho-AMPKα (Thr172) (D79.5E) (Cell Signaling Technology, #4188) was used at 1:1000 to detect active AMPK. Rabbit *Ce*HIF-1 antibody at (1:5,000) was a kind gift from Dr. Peter Ratcliffe, Oxford. Mouse anti-α-tubulin primary antibody (AA4.3, RRID:AB_579793), developed by C. Walsh, was obtained from the Developmental Studies Hybridoma Bank (DSHB), created by the National Institute of Child Health and Human Development (NICHD) of the National Institute of Health (NIH), and maintained at the Department of Biology, University of Iowa. The following secondary antibodies were used: Donkey anti-mouse IgG (H and L) Antibody IRDye 800CW Conjugated (Licor) and Alexa Fluor 680 goat anti-rabbit IgG (H+L) (Invitrogen). LI-COR Image Studio software (RRID:SCR_015795) was used to quantify protein levels in different samples,

relative to α-tubulin levels. Fold change of protein levels was calculated relative to wildtype (N2)/ controls.

ii. Western blot analysis of epithelial cell lines

A549 epithelial cells were lysed in a modified M2 buffer containing 20mM tris[hydroxymethyl]aminomethane, 150mM NaCl at pH 7.4, 0.5% NP40, 3mM EDTA, 3mM EGTA, 4mM PMSF, and a cOmplete Mini, EDTA-free protease inhibitor tablet according to the manufacturer's instructions (Roche, #11836170001). Epithelial cells were collected by mechanical dislodgment in lysis buffer at individual time points, incubated for 20 minutes on ice, and spun at 14,000 x g for 5 minutes to remove insoluble material. 25ug protein was resolved by NuPAGE™ 4-12% Bis-Tris gel (Invitrogen) and transferred to PVDF for immunoblotting. Anti-p53 (Cell Signaling Technology, #9282) and β-actin (DSHB, 224-236-1) primary antibodies were used with HRP-conjugated secondary antibodies to anti-rabbit IgG (Jackson ImmunoResearch, #111-035-003) and anti-mouse IgG (Invitrogen, #62-6520). Densitometry was analyzed with ImageJ software.

RNA extraction and real-time quantitative reverse-transcriptase PCR (RT-PCR)

Worms were bleach-hatched as described above and ~400-800 eggs/plate (2 plates/strain) were seeded on fresh OP50 plates and were allowed to grow (i) for 30-34 hrs. at 25°C or (ii) for 36 hrs. at 20°C and then harvested for RNA extraction. RNA was extracted as described earlier [117]. Briefly, plates were washed with sterile water and centrifuged. Water was carefully removed and 300 µl of Trizol (catalog no. 400753, Life Technologies) was added and snap-frozen immediately in liquid nitrogen. Samples were thawed on ice and then lysed using a Precellys 24 homogenizer (Bertin Corp.). RNA was then purified as detailed with appropriate volumes of reagents modified to 300 µl of Trizol. The RNA pellet was dissolved in 17 µl of RNase-free water. The purified RNA was then treated with deoxyribonuclease using the TURBO DNA-free kit (catalog no. AM1907, Life Technologies) as per the manufacturer's protocol. cDNA was generated by using the iScript

cDNA Synthesis Kit (catalog no. 170–8891, Bio-Rad). qRT-PCR was performed using PowerUp SYBR Green Master Mix (catalog no. A25742, Thermo Fisher Scientific) in QuantStudio 3 Real-Time PCR System (Thermo Fisher Scientific) at a 10 µl sample volume, in a 96-well plate (catalog no. 4346907, Thermo Fisher Scientific). The relative amounts of mRNA were determined using the $\Delta\Delta C_t$ method for quantitation. We selected *pmp-3* as an appropriate internal control for gene expression analysis in *C. elegans*.

All relative changes of mRNA were normalized to either that of the wild-type control or the control for each genotype (specified in figure legends). Each experiment was repeated a minimum of three times. For qPCR reactions, the amplification of a single product with no primer dimers was confirmed by melt-curve analysis performed at the end of the reaction. Primers were designed using Primer3 software and generated by Integrated DNA Technologies. The primers used for the qRT-PCR analysis are listed below:

Gene	**Forward primer (5'-3')**	**Reverse primer (5'-3')**
pfk-1.2	TTGCATCGAATCTGTGAAGC	TCGCTGCAGTCAAAGCTAGA
cyc-2.2	CGGTGGAGCTATTCCAGAAG	GCAACTTGTCCGGATTGTCT
egl-1	TCCAAGCTAGCAGCAATGTG	GCGAAAAAGTCCAGAAGACG
ced-13	GCAACTCAAACACCGTTGAA	CAATGCTGGCATACGTCTTG
phg-1	CAGAGGAGCTTGTACCGACA	TCGTCTCTAGCAGTGCATGT
sod-3	CACTGCTTCAAAGCTTGTTCA	ATGGGAGATCTGGGAGAGTG
mtl-1	TGGATGTAAGGGAGACTGCAA	CATTTTAATGAGCCGCAGCA
lys-7	GCCGTCAAACTTGGCATCTT	GGGTTGTATGCACGAACGAA
pmp-3	TAGAGTCAAGGGTCGCAGTG	ATCGGCACCAAGGAAACTGG
cep-1(a+b isoform)	GCTCACTCTGTCGACTGCTGAGT	AACCCAAGTGTATCTGGGAACTTT

cep-1(a isoform)	GTTGTGCTCGACTCCCAAAAG	GGCACGCTTCTCAATTACAAGTT

Chromatin immunoprecipitation (ChIP)

Chromatin immunoprecipitation (ChIP) was performed as described earlier (Das et al., 2020). Day-one adult worms were bleach-hatched as described above and ~1600 eggs were seeded (~800 eggs/plate and 2 plates/genotype) on fresh OP5O plates. Plates were kept at 25°C for 30-34 hrs. and larvae were washed with 1X PBS (pH 7.4) and cross-linked with freshly prepared 2% formaldehyde (catalog no. 252549, Sigma Aldrich) at room temperature for 10 min followed by addition of 250 mM Tris (pH 7.4) at room temperature for 10 min. Samples were then washed three times in ice-cold 1X PBS supplemented with protease inhibitor cocktail and snap-frozen in liquid nitrogen. The worm pellet was resuspended in FA buffer [50 mM HEPES (pH 7.4), 150 mM NaCl, 50 mM EDTA, 1% Triton-X-100, 0.5% SDS and 0.1% sodium deoxycholate], supplemented with 1 mM DTT and protease inhibitor cocktail. The suspended worm pellet was lysed using a Precellys 24 homogenizer (Bertin Corp.), and then sonicated in a Bioruptor Pico Sonication System (catalog no. B0106001, Diagenode) (15 cycles of 30 s on/off).

Endogenous CEP-1 was immunoprecipitated with anti-FLAG M2 magnetic bead (catalog no. M-8823, Sigma-Aldrich). Beads were first pre-cleared with salmon sperm DNA (catalog no. 15632–011, Invitrogen). Worm lysate was incubated at 4°C overnight with the pre-cleared FLAG beads. Beads were washed with low salt, high salt and LiCl wash buffers and then eluted in buffer containing EDTA, SDS and sodium bicarbonate. The elute was then de-crosslinked overnight in presence of Proteinase K. The DNA was purified by ChIP DNA purification kit (catalog no. D5205, Zymo Research). qPCR analysis of DNA was performed as described above using primer sets specific for different target genes. For all ChIP experiments, 10% of total lysate was used as 'input' and chromatin immunoprecipitated by different antibodies were expressed as % input values. The primers used for ChIP experiments, and the expected amplicon sizes are as follows:

Gene	Position	Forward primer (5'-3')	Reverse primer (5'-3')	Amplicon size
egl-1	TSS +4 to +123)	CTCACCTTTGCCTCAAC CTC	CGAGGAGAAGTCCTG AGACG	120 bp
ced-13	Promoter (-428 to -310)	CTATTCTTGGCCGTGCT CAT	AGGCAATCTAGCATG CACCT	119 bp
phg-1	Promoter -428 to -294)	GCCAAACCTTCCAGA TTTACA	TTCCTAGATAAGGGT TAGATGATGAGA	135 bp
phg-1	Intron 1 (+223 to +326)	AAGCTGAGCTCCGAA AACAA	TTTCCCGCTAAACGA GACAT	104 bp
cki-1	Promoter (-698 to -722)	TTT TCC ATA CTT CAC TAG TCA AAA CCT	GAC AGT GAG AAG CTT TCG TAT TGA	103 bp
cki-1	Promoter (-542 to -428)	TTC CTC ATA ATC ACG GAG CA	GGA ACC GAA GTG GTC AGA TG	114 bp
cki-1	Promoter (-323 to -217)	TCT CCG ACT GCT GAC CT	CGA GAA GGG GTG GAG TCA TA	106 bp

Treatment of mouse epithelial cell lines with human IL-17 and Nutlin3A

A549 epithelial cells were seeded in a 6-well plate overnight and stimulated with 50-100ng/mL recombinant human-IL-17 (Peprotech, SKU 200-17) or 10uM Nutlin3A (Tocris, 675576-98-4), and supernatants and cell lysates were harvested 18 hours later.

QUANTIFICATION AND STATISTICAL ANALYSIS

Each 'experiment' refers to a biological repeat. No statistical methods were used to predetermine sample size. The experiments were not randomized, but some were blinded. The statistical details of experiments could be found in corresponding figure legends. The data were analyzed by using Student's t-test and/or one-way ANOVA with Tukey's correction (GraphPad Prism software) as described in respective figure legends. P values are indicated as follows: *p<0.05; **p< 0.01; ***p<0.001, ns, not significant.

References

1 Cai, L. & Tu, B. P. Driving the cell cycle through metabolism. *Annu Rev Cell Dev Biol* **28**, 59-87, doi:10.1146/annurev-cellbio-092910-154010 (2012).

2 Wang, A., Luan, H. H. & Medzhitov, R. An evolutionary perspective on immunometabolism. *Science* **363**, doi:10.1126/science.aar3932 (2019).

3 Lee, I. H. & Finkel, T. Metabolic regulation of the cell cycle. *Curr Opin Cell Biol* **25**, 724-729, doi:10.1016/j.ceb.2013.07.002 (2013).

4 Hall, P. A. & Lane, D. P. Tumor suppressors: a developing role for p53? *Curr Biol* **7**, R144-147, doi:10.1016/s0960-9822(97)70074-5 (1997).

5 Levine, A. J. p53: 800 million years of evolution and 40 years of discovery. *Nat Rev Cancer* **20**, 471-480, doi:10.1038/s41568-020-0262-1 (2020).

6 Zhu, J. & Thompson, C. B. Metabolic regulation of cell growth and proliferation. *Nat Rev Mol Cell Biol* **20**, 436-450, doi:10.1038/s41580-019-0123-5 (2019).

7 Altan-Bonnet, G. & Mukherjee, R. Cytokine-mediated communication: a quantitative appraisal of immune complexity. *Nat Rev Immunol* **19**, 205-217, doi:10.1038/s41577-019-0131-x (2019).

8 Talbot, S., Foster, S. L. & Woolf, C. J. Neuroimmunity: Physiology and Pathology. *Annu Rev Immunol* **34**, 421-447, doi:10.1146/annurev-immunol-041015-055340 (2016).

9 Mills, K. H. G. IL-17 and IL-17-producing cells in protection versus pathology. *Nat Rev Immunol*, doi:10.1038/s41577-022-00746-9 (2022).

10 Li, X., Bechara, R., Zhao, J., McGeachy, M. J. & Gaffen, S. L. IL-17 receptor-based signaling and implications for disease. *Nat Immunol* **20**, 1594-1602, doi:10.1038/s41590-019-0514-y (2019).

11 McGeachy, M. J., Cua, D. J. & Gaffen, S. L. The IL-17 Family of Cytokines in Health and Disease. *Immunity* **50**, 892-906, doi:10.1016/j.immuni.2019.03.021 (2019).

12 Choi, G. B. *et al.* The maternal interleukin-17a pathway in mice promotes autism-like phenotypes in offspring. *Science* **351**, 933-939, doi:10.1126/science.aad0314 (2016).

13 Reed, M. D. *et al.* IL-17a promotes sociability in mouse models of neurodevelopmental disorders. *Nature* **577**, 249-253, doi:10.1038/s41586-019-1843-6 (2020).

14 Chen, C. *et al.* IL-17 is a neuromodulator of Caenorhabditis elegans sensory responses. *Nature* **542**, 43-48, doi:10.1038/nature20818 (2017).

15 Flynn, S. M. *et al.* MALT-1 mediates IL-17 neural signaling to regulate C. elegans behavior, immunity and longevity. *Nat Commun* **11**, 2099, doi:10.1038/s41467-020-15872-y (2020).

16 Lillis, M., Zaccardi, N. J. & Heiman, M. G. Axon-dendrite and apical-basolateral sorting in a single neuron. *Genetics* **221**, doi:10.1093/genetics/iyac036 (2022).

17 Low, I. I. C. *et al.* Morphogenesis of neurons and glia within an epithelium. *Development* **146**, doi:10.1242/dev.171124 (2019).

18 Jain, A. K. & Barton, M. C. p53: emerging roles in stem cells, development and beyond. *Development* **145**, doi:10.1242/dev.158360 (2018).

19 Rutkowski, R., Hofmann, K. & Gartner, A. Phylogeny and function of the invertebrate p53 superfamily. *Cold Spring Harb Perspect Biol* **2**, a001131, doi:10.1101/cshperspect.a001131 (2010).

20 Bowling, S. *et al.* P53 and mTOR signalling determine fitness selection through cell competition during early mouse embryonic development. *Nat Commun* **9**, 1763, doi:10.1038/s41467-018-04167-y (2018).

21 Zhang, G. *et al.* p53 pathway is involved in cell competition during mouse embryogenesis. *Proc Natl Acad Sci U S A* **114**, 498-503, doi:10.1073/pnas.1617414114 (2017).

22 Hong, H. *et al.* Suppression of induced pluripotent stem cell generation by the p53-p21 pathway. *Nature* **460**, 1132-1135, doi:10.1038/nature08235 (2009).

23 Liu, Y., Hoya-Arias, R. & Nimer, S. D. The role of p53 in limiting somatic cell reprogramming. *Cell Res* **19**, 1227-1228, doi:10.1038/cr.2009.121 (2009).

1280 24 Lu, W. J., Amatruda, J. F. & Abrams, J. M. p53 ancestry: gazing through an evolutionary
1281 lens. *Nat Rev Cancer* **9**, 758-762, doi:10.1038/nrc2732 (2009).
1282 25 Hu, P. J. Dauer. *WormBook*, 1-19, doi:10.1895/wormbook.1.144.1 (2007).
1283 26 Karp, X. Working with dauer larvae. *WormBook* **2018**, 1-19,
1284 doi:10.1895/wormbook.1.180.1 (2018).
1285 27 Ewald, C. Y., Landis, J. N., Porter Abate, J., Murphy, C. T. & Blackwell, T. K. Dauer-
1286 independent insulin/IGF-1-signalling implicates collagen remodelling in longevity. *Nature*
1287 **519**, 97-101, doi:10.1038/nature14021 (2015).
1288 28 Burnell, A. M., Houthoofd, K., O'Hanlon, K. & Vanfleteren, J. R. Alternate metabolism
1289 during the dauer stage of the nematode Caenorhabditis elegans. *Exp Gerontol* **40**, 850-
1290 856, doi:10.1016/j.exger.2005.09.006 (2005).
1291 29 Holt, S. J. Staying alive in adversity: transcriptome dynamics in the stress-resistant dauer
1292 larva. *Funct Integr Genomics* **6**, 285-299, doi:10.1007/s10142-006-0024-5 (2006).
1293 30 Lee, J. S. *et al.* FMRFamide-like peptides expand the behavioral repertoire of a densely
1294 connected nervous system. *Proc Natl Acad Sci U S A* **114**, E10726-E10735,
1295 doi:10.1073/pnas.1710374114 (2017).
1296 31 Schaedel, O. N., Gerisch, B., Antebi, A. & Sternberg, P. W. Hormonal signal amplification
1297 mediates environmental conditions during development and controls an irreversible
1298 commitment to adulthood. *PLoS Biol* **10**, e1001306, doi:10.1371/journal.pbio.1001306
1299 (2012).
1300 32 Wang, J. & Kim, S. K. Global analysis of dauer gene expression in Caenorhabditis
1301 elegans. *Development* **130**, 1621-1634, doi:10.1242/dev.00363 (2003).
1302 33 Wirick, M. J. *et al.* daf-16/FOXO blocks adult cell fate in Caenorhabditis elegans dauer
1303 larvae via lin-41/TRIM71. *PLoS Genet* **17**, e1009881, doi:10.1371/journal.pgen.1009881
1304 (2021).

34 Alcantar-Fernandez, J., Navarro, R. E., Salazar-Martinez, A. M., Perez-Andrade, M. E. & Miranda-Rios, J. Caenorhabditis elegans respond to high-glucose diets through a network of stress-responsive transcription factors. *PLoS One* **13**, e0199888, doi:10.1371/journal.pone.0199888 (2018).

35 Franco-Juarez, B. *et al.* Effects of High Dietary Carbohydrate and Lipid Intake on the Lifespan of C. elegans. *Cells* **10**, doi:10.3390/cells10092359 (2021).

36 Garcia, A. M. *et al.* Glucose induces sensitivity to oxygen deprivation and modulates insulin/IGF-1 signaling and lipid biosynthesis in Caenorhabditis elegans. *Genetics* **200**, 167-184, doi:10.1534/genetics.115.174631 (2015).

37 Missios, P. *et al.* Glucose substitution prolongs maintenance of energy homeostasis and lifespan of telomere dysfunctional mice. *Nat Commun* **5**, 4924, doi:10.1038/ncomms5924 (2014).

38 Mondoux, M. A. *et al.* O-linked-N-acetylglucosamine cycling and insulin signaling are required for the glucose stress response in Caenorhabditis elegans. *Genetics* **188**, 369-382, doi:10.1534/genetics.111.126490 (2011).

39 Schlotterer, A. *et al.* C. elegans as model for the study of high glucose- mediated life span reduction. *Diabetes* **58**, 2450-2456, doi:10.2337/db09-0567 (2009).

40 Zarse, K. *et al.* Impaired insulin/IGF1 signaling extends life span by promoting mitochondrial L-proline catabolism to induce a transient ROS signal. *Cell Metab* **15**, 451-465, doi:10.1016/j.cmet.2012.02.013 (2012).

41 Wu, Z. *et al.* Dietary Restriction Extends Lifespan through Metabolic Regulation of Innate Immunity. *Cell Metab* **29**, 1192-1205 e1198, doi:10.1016/j.cmet.2019.02.013 (2019).

42 Feng, Y., Williams, B. G., Koumanov, F., Wolstenholme, A. J. & Holman, G. D. FGT-1 is the major glucose transporter in C. elegans and is central to aging pathways. *Biochem J* **456**, 219-229, doi:10.1042/BJ20131101 (2013).

43 Kenyon, C., Chang, J., Gensch, E., Rudner, A. & Tabtiang, R. A C. elegans mutant that lives twice as long as wild type. *Nature* **366**, 461-464, doi:10.1038/366461a0 (1993).

44 Ogg, S. *et al.* The Fork head transcription factor DAF-16 transduces insulin-like metabolic and longevity signals in C. elegans. *Nature* **389**, 994-999, doi:10.1038/40194 (1997).

45 Henderson, S. T. & Johnson, T. E. daf-16 integrates developmental and environmental inputs to mediate aging in the nematode Caenorhabditis elegans. *Curr Biol* **11**, 1975-1980, doi:10.1016/s0960-9822(01)00594-2 (2001).

46 Johnson, T. E. *et al.* Longevity genes in the nematode Caenorhabditis elegans also mediate increased resistance to stress and prevent disease. *J Inherit Metab Dis* **25**, 197-206, doi:10.1023/a:1015677828407 (2002).

47 Tissenbaum, H. A. & Ruvkun, G. An insulin-like signaling pathway affects both longevity and reproduction in Caenorhabditis elegans. *Genetics* **148**, 703-717, doi:10.1093/genetics/148.2.703 (1998).

48 Ritter, A. D. *et al.* Complex expression dynamics and robustness in C. elegans insulin networks. *Genome Res* **23**, 954-965, doi:10.1101/gr.150466.112 (2013).

49 Chen, Y. & Baugh, L. R. Ins-4 and daf-28 function redundantly to regulate C. elegans L1 arrest. *Dev Biol* **394**, 314-326, doi:10.1016/j.ydbio.2014.08.002 (2014).

50 Pierce, S. B. *et al.* Regulation of DAF-2 receptor signaling by human insulin and ins-1, a member of the unusually large and diverse C. elegans insulin gene family. *Genes Dev* **15**, 672-686, doi:10.1101/gad.867301 (2001).

51 Brunton, J., Steele, S., Ziehr, B., Moorman, N. & Kawula, T. Feeding uninvited guests: mTOR and AMPK set the table for intracellular pathogens. *PLoS Pathog* **9**, e1003552, doi:10.1371/journal.ppat.1003552 (2013).

52 Schulz, T. J. *et al.* Glucose restriction extends Caenorhabditis elegans life span by inducing mitochondrial respiration and increasing oxidative stress. *Cell Metab* **6**, 280-293, doi:10.1016/j.cmet.2007.08.011 (2007).

53 Carman, L., Schuck, R. J., Li, E. & Nelson, M. D. An AMPK biosensor for Caenorhabditis elegans. *MicroPubl Biol* **2022**, doi:10.17912/micropub.biology.000596 (2022).

54 Zecic, A. & Braeckman, B. P. DAF-16/FoxO in Caenorhabditis elegans and Its Role in Metabolic Remodeling. *Cells* **9**, doi:10.3390/cells9010109 (2020).

55 Oh, S. W. *et al.* JNK regulates lifespan in Caenorhabditis elegans by modulating nuclear translocation of forkhead transcription factor/DAF-16. *Proc Natl Acad Sci U S A* **102**, 4494-4499, doi:10.1073/pnas.0500749102 (2005).

56 Greer, E. L. *et al.* An AMPK-FOXO pathway mediates longevity induced by a novel method of dietary restriction in C. elegans. *Curr Biol* **17**, 1646-1656, doi:10.1016/j.cub.2007.08.047 (2007).

57 Leiser, S. F., Begun, A. & Kaeberlein, M. HIF-1 modulates longevity and healthspan in a temperature-dependent manner. *Aging Cell* **10**, 318-326, doi:10.1111/j.1474-9726.2011.00672.x (2011).

58 Chen, D., Thomas, E. L. & Kapahi, P. HIF-1 modulates dietary restriction-mediated lifespan extension via IRE-1 in Caenorhabditis elegans. *PLoS Genet* **5**, e1000486, doi:10.1371/journal.pgen.1000486 (2009).

59 Paek, J. *et al.* Mitochondrial SKN-1/Nrf mediates a conserved starvation response. *Cell Metab* **16**, 526-537, doi:10.1016/j.cmet.2012.09.007 (2012).

60 Gurkar, A. U. *et al.* Dysregulation of DAF-16/FOXO3A-mediated stress responses accelerates oxidative DNA damage induced aging. *Redox Biol* **18**, 191-199, doi:10.1016/j.redox.2018.06.005 (2018).

61 Perrin, A. J. *et al.* Noncanonical control of C. elegans germline apoptosis by the insulin/IGF-1 and Ras/MAPK signaling pathways. *Cell Death Differ* **20**, 97-107, doi:10.1038/cdd.2012.101 (2013).

62 Quevedo, C., Kaplan, D. R. & Derry, W. B. AKT-1 regulates DNA-damage-induced germline apoptosis in C. elegans. *Curr Biol* **17**, 286-292, doi:10.1016/j.cub.2006.12.038 (2007).

63 Baruah, A. *et al.* CEP-1, the Caenorhabditis elegans p53 homolog, mediates opposing longevity outcomes in mitochondrial electron transport chain mutants. *PLoS Genet* **10**, e1004097, doi:10.1371/journal.pgen.1004097 (2014).

64 Yanase, S., Suda, H., Yasuda, K. & Ishii, N. Impaired p53/CEP-1 is associated with lifespan extension through an age-related imbalance in the energy metabolism of C. elegans. *Genes Cells* **22**, 1004-1010, doi:10.1111/gtc.12540 (2017).

65 Derry, W. B., Putzke, A. P. & Rothman, J. H. Caenorhabditis elegans p53: role in apoptosis, meiosis, and stress resistance. *Science* **294**, 591-595, doi:10.1126/science.1065486 (2001).

66 Levi-Ferber, M. *et al.* It's all in your mind: determining germ cell fate by neuronal IRE-1 in C. elegans. *PLoS Genet* **10**, e1004747, doi:10.1371/journal.pgen.1004747 (2014).

67 Hicks, T. *et al.* R-loop-induced irreparable DNA damage evades checkpoint detection in the C. elegans germline. *Nucleic Acids Res* **50**, 8041-8059, doi:10.1093/nar/gkac621 (2022).

68 Schumacher, B. *et al.* Translational repression of C. elegans p53 by GLD-1 regulates DNA damage-induced apoptosis. *Cell* **120**, 357-368, doi:10.1016/j.cell.2004.12.009 (2005).

69 Arum, O. & Johnson, T. E. Reduced expression of the Caenorhabditis elegans p53 ortholog cep-1 results in increased longevity. *J Gerontol A Biol Sci Med Sci* **62**, 951-959, doi:10.1093/gerona/62.9.951 (2007).

70 Lee, C. C. *et al.* Mutation of a Nopp140 gene dao-5 alters rDNA transcription and increases germ cell apoptosis in C. elegans. *Cell Death Dis* **5**, e1158, doi:10.1038/cddis.2014.114 (2014).

71 Gartner, A., Boag, P. R. & Blackwell, T. K. Germline survival and apoptosis. *WormBook*, 1-20, doi:10.1895/wormbook.1.145.1 (2008).

72 Greiss, S., Schumacher, B., Grandien, K., Rothblatt, J. & Gartner, A. Transcriptional profiling in C. elegans suggests DNA damage dependent apoptosis as an ancient function of the p53 family. *BMC Genomics* **9**, 334, doi:10.1186/1471-2164-9-334 (2008).

73 Schumacher, B. *et al.* C. elegans ced-13 can promote apoptosis and is induced in response to DNA damage. *Cell Death Differ* **12**, 153-161, doi:10.1038/sj.cdd.4401539 (2005).

74 Schertel, C. & Conradt, B. C. elegans orthologs of components of the RB tumor suppressor complex have distinct pro-apoptotic functions. *Development* **134**, 3691-3701, doi:10.1242/dev.004606 (2007).

75 Rasmussen, M. A. *et al.* Transient p53 suppression increases reprogramming of human fibroblasts without affecting apoptosis and DNA damage. *Stem Cell Reports* **3**, 404-413, doi:10.1016/j.stemcr.2014.07.006 (2014).

76 Sendoel, A., Kohler, I., Fellmann, C., Lowe, S. W. & Hengartner, M. O. HIF-1 antagonizes p53-mediated apoptosis through a secreted neuronal tyrosinase. *Nature* **465**, 577-583, doi:10.1038/nature09141 (2010).

77 Karp, X. & Greenwald, I. Control of cell-fate plasticity and maintenance of multipotency by DAF-16/FoxO in quiescent Caenorhabditis elegans. *Proc Natl Acad Sci U S A* **110**, 2181-2186, doi:10.1073/pnas.1222377110 (2013).

78 Tenen, C. C. & Greenwald, I. Cell Non-autonomous Function of daf-18/PTEN in the Somatic Gonad Coordinates Somatic Gonad and Germline Development in C. elegans Dauer Larvae. *Curr Biol* **29**, 1064-1072 e1068, doi:10.1016/j.cub.2019.01.076 (2019).

79 Hand, S. C., Denlinger, D. L., Podrabsky, J. E. & Roy, R. Mechanisms of animal diapause: recent developments from nematodes, crustaceans, insects, and fish. *Am J Physiol Regul Integr Comp Physiol* **310**, R1193-1211, doi:10.1152/ajpregu.00250.2015 (2016).

80 Hong, Y., Roy, R. & Ambros, V. Developmental regulation of a cyclin-dependent kinase inhibitor controls postembryonic cell cycle progression in Caenorhabditis elegans. *Development* **125**, 3585-3597, doi:10.1242/dev.125.18.3585 (1998).

81 Koreth, J. & van den Heuvel, S. Cell-cycle control in Caenorhabditis elegans: how the worm moves from G1 to S. *Oncogene* **24**, 2756-2764, doi:10.1038/sj.onc.1208607 (2005).

82 Liu, Y. *et al.* p53 regulates hematopoietic stem cell quiescence. *Cell Stem Cell* **4**, 37-48, doi:10.1016/j.stem.2008.11.006 (2009).

83 Cheung, T. H. & Rando, T. A. Molecular regulation of stem cell quiescence. *Nat Rev Mol Cell Biol* **14**, 329-340, doi:10.1038/nrm3591 (2013).

84 Vousden, K. H. & Ryan, K. M. p53 and metabolism. *Nat Rev Cancer* **9**, 691-700, doi:10.1038/nrc2715 (2009).

85 Roy, S. H. *et al.* A complex regulatory network coordinating cell cycles during C. elegans development is revealed by a genome-wide RNAi screen. *G3 (Bethesda)* **4**, 795-804, doi:10.1534/g3.114.010546 (2014).

86 Derry, W. B. *et al.* Regulation of developmental rate and germ cell proliferation in Caenorhabditis elegans by the p53 gene network. *Cell Death Differ* **14**, 662-670, doi:10.1038/sj.cdd.4402075 (2007).

87 Pinkston-Gosse, J. & Kenyon, C. DAF-16/FOXO targets genes that regulate tumor growth in Caenorhabditis elegans. *Nat Genet* **39**, 1403-1409, doi:10.1038/ng.2007.1 (2007).

88 Del Sal, G., Ruaro, M. E., Philipson, L. & Schneider, C. The growth arrest-specific gene, gas1, is involved in growth suppression. *Cell* **70**, 595-607, doi:10.1016/0092-8674(92)90429-g (1992).

89 Del Sal, G. *et al.* Gas1-induced growth suppression requires a transactivation-independent p53 function. *Mol Cell Biol* **15**, 7152-7160, doi:10.1128/MCB.15.12.7152 (1995).

90 Segovia, J. & Zarco, N. Gas1 is a pleiotropic regulator of cellular functions: from embryonic development to molecular actions in cancer gene therapy. *Mini Rev Med Chem* **14**, 1139-1147, doi:10.2174/1389557514666141127142301 (2014).

91 Walker, M. D. *et al.* WormPaths: Caenorhabditis elegans metabolic pathway annotation and visualization. *Genetics* **219**, doi:10.1093/genetics/iyab089 (2021).

92 Chen, K. *et al.* IL-17 Receptor Signaling in the Lung Epithelium Is Required for Mucosal Chemokine Gradients and Pulmonary Host Defense against K. pneumoniae. *Cell Host Microbe* **20**, 596-605, doi:10.1016/j.chom.2016.10.003 (2016).

93 Jones, R. G. *et al.* AMP-activated protein kinase induces a p53-dependent metabolic checkpoint. *Mol Cell* **18**, 283-293, doi:10.1016/j.molcel.2005.03.027 (2005).

94 Das, S., Min, S. & Prahlad, V. Gene bookmarking by the heat shock transcription factor programs the insulin-like signaling pathway. *Mol Cell* **81**, 4843-4860 e4848, doi:10.1016/j.molcel.2021.09.022 (2021).

95 Das, S. *et al.* Serotonin signaling by maternal neurons upon stress ensures progeny survival. *Elife* **9**, doi:10.7554/eLife.55246 (2020).

96 Tatum, M. C. *et al.* Neuronal serotonin release triggers the heat shock response in C. elegans in the absence of temperature increase. *Curr Biol* **25**, 163-174, doi:10.1016/j.cub.2014.11.040 (2015).

97 Ooi, F. K. & Prahlad, V. Olfactory experience primes the heat shock transcription factor HSF-1 to enhance the expression of molecular chaperones in C. elegans. *Sci Signal* **10**, doi:10.1126/scisignal.aan4893 (2017).

98 Venkatesh, H. & Monje, M. Neuronal Activity in Ontogeny and Oncology. *Trends Cancer* **3**, 89-112, doi:10.1016/j.trecan.2016.12.008 (2017).

99 Curry, R. N. & Glasgow, S. M. The Role of Neurodevelopmental Pathways in Brain Tumors. *Front Cell Dev Biol* **9**, 659055, doi:10.3389/fcell.2021.659055 (2021).

100 Cully, M. Cancer: Targeting IL-17 in pancreatic cancer. *Nat Rev Drug Discov* **13**, 493, doi:10.1038/nrd4372 (2014).

101 Philip, M., Rowley, D. A. & Schreiber, H. Inflammation as a tumor promoter in cancer induction. *Semin Cancer Biol* **14**, 433-439, doi:10.1016/j.semcancer.2004.06.006 (2004).

102 Bordon, Y. Signalling: a new master to rival NF-kappaB? *Nat Rev Immunol* **14**, 432, doi:10.1038/nri3708 (2014).

103 Gibson, D. G. *et al.* Enzymatic assembly of DNA molecules up to several hundred kilobases. *Nat Methods* **6**, 343-345, doi:10.1038/nmeth.1318 (2009).

104 Nonet, M. L. *et al.* Caenorhabditis elegans rab-3 mutant synapses exhibit impaired function and are partially depleted of vesicles. *J Neurosci* **17**, 8061-8073 (1997).

105 Nika, L., Gibson, T., Konkus, R. & Karp, X. Fluorescent Beads Are a Versatile Tool for Staging Caenorhabditis elegans in Different Life Histories. *G3 (Bethesda)* **6**, 1923-1933, doi:10.1534/g3.116.030163 (2016).

106 Krueger, F. (2021).

107 Kopylova, E., Noe, L. & Touzet, H. SortMeRNA: fast and accurate filtering of ribosomal RNAs in metatranscriptomic data. *Bioinformatics* **28**, 3211-3217, doi:10.1093/bioinformatics/bts611 (2012).

108 Yates, A. D. *et al.* Ensembl Genomes 2022: an expanding genome resource for non-vertebrates. *Nucleic Acids Res* **50**, D996-D1003, doi:10.1093/nar/gkab1007 (2022).

109 Dobin, A. *et al.* STAR: ultrafast universal RNA-seq aligner. *Bioinformatics* **29**, 15-21, doi:10.1093/bioinformatics/bts635 (2013).

110 Liao, Y., Smyth, G. K. & Shi, W. The R package Rsubread is easier, faster, cheaper and better for alignment and quantification of RNA sequencing reads. *Nucleic Acids Research* **47**, e47-e47, doi:10.1093/nar/gkz114 (2019).

111 Love, M. I., Huber, W. & Anders, S. Moderated estimation of fold change and dispersion for RNA-seq data with DESeq2. *Genome Biol* **15**, 550, doi:10.1186/s13059-014-0550-8 (2014).

112 Davis, P. *et al.* WormBase in 2022-data, processes, and tools for analyzing Caenorhabditis elegans. *Genetics* **220**, doi:10.1093/genetics/iyac003 (2022).

113 Wu, T. *et al.* clusterProfiler 4.0: A universal enrichment tool for interpreting omics data. *Innovation (N Y)* **2**, 100141, doi:10.1016/j.xinn.2021.100141 (2021).

114 Carlson, M. (2019).

115 Kanehisa, M., Furumichi, M., Sato, Y., Kawashima, M. & Ishiguro-Watanabe, M. KEGG for taxonomy-based analysis of pathways and genomes. *Nucleic Acids Res*, doi:10.1093/nar/gkac963 (2022).

116 Gu, Z. Complex heatmap visualization. *iMeta* **1**, e43, doi:https://doi.org/10.1002/imt2.43 (2022).

117 Chikka, M. R., Anbalagan, C., Dvorak, K., Dombeck, K. & Prahlad, V. The Mitochondria-Regulated Immune Pathway Activated in the C. elegans Intestine Is Neuroprotective. *Cell Rep* **16**, 2399-2414, doi:10.1016/j.celrep.2016.07.077 (2016).